PB2001-101409

FACTORS THAT AFFECT GENERATION OF COOLANT MISTS

David Leith, Principal Investigator
Jonathan Thornburg, Co-Invesitgator
Department of Environmental Sciences and Engineering
Rosenau Hall, CB 7400
University of North Carolina, Chapel Hill, NC 27599

NIOSH Grant R01 0H03293-02
Roy Fleming, Project Director

December 14, 1998

TALBE OF CONTENTS

LIST OF ABBREVIATIONS

ACRONYMS

ACGIH	American Conference of Governmental Industrial Hygienists
API	Amherst Process Instruments
GC-MS	gas chromatograph-mass spectrometer
GSD	geometric standard deviation
MMD	mass median diameter
NIOSH	National Institute for Occupational Safety and Health
OSHA	Occupational Safety and Health Administration
PEL	permissable exposure level
PMT	photomultiplier tube voltage
SMD	Sauter mean diameter
TLV	threshold limit value

SYMBOLS

C	cut depth (mm)
C_p	Specific heat (J/g-K)
D	metal rod diameter (cm)
d, d_p	drop diameter (μm)
F	feed rate (cm/rev)
G	Mist generation rate (mg/s)
H_{cap}	heat capacity (J/g)
H_{vap}	heat of vaporization (J/g)

K	dimensionless parameter
M	dimensionless mist generation number
Oh	Ohnesorge number
Q_f	fluid flow (cm^3/s)
Q_m	metal removal rate (cm^3/s)
Re	Reynolds number
T_{BP}	boiling temperature (°C)
T_o	ambient temperature (°C)
V_j	jet velocity (cm/s)
V_t	tangential velocity (cm/s)
v	drop velocity (cm/s)
We	Weber number
ρ	fluid density (g/cm^3)
σ	fluid surface tension (dynes/cm)
ω	rotational speed (rev/s)

LIST OF TABLES

LIST OF FIGURES

SIGNIFICANT FINDINGS

Of the three formation mechanisms identified during this research, impaction was the least significant source of mist. The mist generation rate was proportional to the fluid flow. The mass median diameter of the mist produced by impaction increased as the metalworking fluid viscosity increased. During these experiments, mass median diameters produced by impaction were larger than 6 μm.

The centrifugal force generated by the rotating workpiece was the second most important source of mist, and produced the largest particles. The number of particles generated depended on the rotational speed of the workpiece, fluid flow, and their interaction term. Rotational speed, fluid flow, and fluid type influenced the mass median diameter of the mist. Typical mass median diameters were between 40 and 100 μm. The complex interaction between the rotational speed and fluid flow on the size distribution can be understood by plotting the mass median diameter versus the dimensionless ratio, V_j/V_t. V_j is the application velocity of the metalworking fluid and V_t is the tangential velocity of the drops generated by the rotating workpiece. The measured size distribution resulted from the atomization of the fluid by the rotating workpiece, and the collision of these droplets with the housing walls.

The most important source of metalworking fluid mist was the evaporation/ condensation process. The heat generated by the machining process evaporated the metalworking fluid. As the vapors moved away from the heat source, they condensed to form mist drops. Evaporation/condensation generated more than 100 to 1000 times more mist drops than impaction or centrifugal force. Using a water-based fluid instead of straight oil, increasing the metalworking fluid flow, or reducing the machining rate reduced the amount mist generated. The machining rate was determined by the rotational speed and cut depth. The ratio of the volumetric metal removal rate to the fluid flow, defined as the mist generation number, was developed to empirically determine the mist generation rate. The mist generation number accounts for the heat generated during machining and the transfer of this heat to the metalworking fluid. In general, evaporation/condensation produced smaller drops than the other mechanisms. The mass median diameter of the mist generated by evaporation/condensation was less than 3 μm, and the size distribution of the mist was not influenced by any machining or fluid parameters. The condensation rate, drop coagulation, and continuous vapor generation probably affected the mist size distribution. Because so many small particles were generated, evaporation/condensation poses the largest threat to worker's health.

USEFULNESS OF FINDINGS

Prevention of Mist Formation

Based on the results from these experiments, industrial facilities can decrease the mist generation rate by preventing evaporation/condensation of the metalworking fluid from occurring. To accomplish this task, the amount of heat the metalworking fluid can absorb must be increased or the amount of heat generated during machining must be decreased. Increasing metalworking fluid flow or using a water-based fluid would increase the amount of heat that could be absorbed per unit mass of metalworking fluid. To decrease the amount of heat generated, the rotational speed and depth of cut must be reduced. However, all of these options would alter the production process, and decrease the production rate. Changes in the production process may increase operating costs through higher metalworking fluid usage, increased tool wear, and diminished surface finish quality; whereas slower production rates would decrease revenue.

In addition, altering machining and fluid parameters would affect the amount of mist generated by centrifugal force and impaction. A slower rotational speed would decrease the amount of mist generated by centrifugal force, and higher flows would make impaction a more important mechanism.

The feasibility of achieving the recommended metalworking fluid mist PEL through pollution prevention must be assessed by individual facilities. Larger facilities would have to perform a cost-benefit analysis to determine if the savings from reduced health care expenses and not purchasing mist collectors would offset increased production costs resulting from altered production processes. However smaller, "mom & pop" machine shops may be able to reduce metalworking fluid mist concentrations using pollution prevention because their machining rate may be more flexible. This situation is amenable to reducing the mist generation rate through slower machining rates and increased fluid flow.

Increasing Drop Size

The other option a facility has for reducing mist concentrations is to increase the drop size. For a facility that decides to reduce metalworking fluid mist concentrations using mist collectors, keeping the mist drops as large as possible will improve mist collector efficiency. Although altering machining or fluid parameters will not affect the mist size distribution generated by evaporation/condensation, enclosing machines and installing local exhaust ventilation will maintain a high vapor concentration and prevent evaporation of the drops generated by the machining process.

ABSTRACT

Metalworking fluids are used as coolants and lubricants during metal machining. The splashing of the fluid, centrifugal force generated by the rotating surface, and heat generated by the machining result in a mist that is associated with several adverse health effects. Previous studies have investigated mist size distributions and concentrations in industrial facilities. However, these studies did not examine the effect of all the machining and metalworking fluid parameters affecting the mist formation process.

The goal of this research was to characterize the mist formation process. The salient machining and metalworking fluid parameters affecting the mist generation rate and size distribution of each mist formation mechanism were identified. When appropriate, empirical equations predicting the mist generation rate or size distribution were developed.

Of the three formation mechanisms, impaction generated the least amount of mist. The generation rate was determined by fluid flow, and the mass median diameter of the size distribution was influenced by fluid viscosity. Centrifugal force was the second most important formation mechanism and generated the largest drops. The rotational speed of the workpiece and fluid flow affected the mist generation rate. Typical mass median diameters produced by centrifugal force ranged from 5 to 120 μm, depending on the type metalworking fluid, fluid flow, and rotational speed of the workpiece. The heat generated by the machining process resulted in the generation of 100 to 1000 times more mist than impaction or

centrifugal force. The mist generation rate depended on the amount of heat produced during machining and the heat absorption capacity of the metalworking fluid. Cut depth and rotational speed determined the amount of heat generated; whereas the type of metalworking fluid and fluid flow specified the heat absorption capacity. These parameters were combined into a dimensionless mist generation number that predicted the mist generation rate. The size distribution of the mist generated depended solely on the type of metalworking fluid. The condensation rate, coagulation of drops, and the constantly changing environment within experimental apparatus probably determined the mist size distribution.

I. INTRODUCTION

A. Specific Aims

Metalworking fluids are commonly used in the metal machining industry as coolants and lubricants. The application method of the metalworking fluid, the centrifugal force produced by the rotating tool or workpiece, and the heat produced by the machining process generate a mist with drop diameters in the thoracic and respirable size ranges. Mist drops in these size ranges are associated with a variety of adverse health effects in exposed workers.

Machine enclosures, local exhaust ventilation, and mist collectors are currently used to reduce the health and safety hazards to exposed workers. However, these options are expensive and do not effectively remove sub-micron mist drops. Preventing mist from being generated or increasing the diameter of the mist drops is an alternative, more basic means for minimizing exposure to mists. However, both options require a comprehensive understanding of the mist formation process. At present, research concerning mist formation is limited, and the formation mechanisms are poorly understood. Therefore, the goal of this research is to:

> **Characterize the factors that influence the mist generation rate and size distribution during metal machining.**

To achieve this goal, the following objectives will be met.

1. Determine the relative importance of the mist formation mechanisms. The formation mechanisms will be identified, and the contribution of each mechanism to the mist generation rate and size distribution will be quantitatively determined.

2. Identify the salient factors in the mist formation process. Potentially salient parameters will be determined, and experiments will be conducted to ascertain which factors influence the mist generation rate and size distribution.

3. Develop mathematical expressions estimating the generation rate and size distribution of the mist. Empirical equations for calculating the size distribution and generation rate will be developed using dimensionless groups combining the important variables.

Concepts developed from this research can be used by industrial facilities to eliminate or reduce exposures to mists. This study will establish how changing machining parameters reduces the mist generation rate, and increases the size of the mist drops. Minimizing the generation rate and increasing the drop diameter will reduce worker exposure to inhalable particles. In addition, the empirical models developed through this research will aid in epidemiological studies where exposure measurements are incomplete by providing a method for estimating exposure levels without collecting personal or ambient samples.

B. Purpose and Types of Metalworking Fluids

Metalworking fluids have been used as coolants and lubricants during metal machining for more than two centuries, but became widely employed when Northcott documented increased production in machining operations through their use (Springborn, 1967). The production rate increases because the metalworking fluid cools the tool used to machine the workpiece and lubricates the tool-workpiece interface (Frazier, 1982). The metalworking fluid cools the tool by removing the metal chips formed during the cutting process. Approximately 80% of the heat generated by the cutting action is absorbed by the chips (Leep, 1994). Flooding the machining area with a metalworking fluid cools the tool and flushes chips away from the machining site, thereby prolonging tool life and allowing faster cutting speeds (Booser, 1984). The metalworking fluid also reduces the friction between the tool and the workpiece, thus increasing tool life and improving the surface finish on the workpiece (Frazier, 1982; Leep, 1994).

Three types of metalworking fluids are available commercially. Straight oils are the most common, but soluble and synthetic oils are increasing in popularity because of their lower cost (Leep, 1994).

Straight oil, also known as insoluble oil, is derived from animal, vegetable, or mineral (petroleum) sources. Straight oil is comprised mainly of alkanes, but also may contain other organic compounds such as polycyclic aromatic hydrocarbons (Konrad *et al.*, 1991). Supplements such as sulfur, chlorine, and phosphorous can be added to improve the lubrication and heat dissipation capabilities of the straight oil (Booser, 1984).

Another type of metalworking fluid is soluble oil. Soluble oil also is called emulsified oil because of the oil-water emulsion that is formed. Soluble oil contains small concentrations (5% to 20% by volume) of a straight oil mixed with water and an emulsifier, usually a sulfonate (Byers, 1994). The presence of water in soluble oil requires additional chemicals to prevent bacterial growth and inhibit rust formation (Frazier, 1982).

Finally, synthetic and semi-synthetic fluids are the newest types of metalworking fluids. Synthetic fluids are mixtures of organic or inorganic salts and water (Booser, 1984). Semi-synthetic fluids are similar, but contain trace amounts (< 1%) of straight oil (Springborn, 1967). Both synthetic and semi-synthetic fluids offer good microbial control, lubrication properties, and rust control. Wetting agents are typically added to increase the lubrication properties of the fluid for use under extreme pressure conditions (Booser, 1984).

C. Health Effects and Exposure Levels

In 1989 there were more than 1.8 million metal cutting machines operating in the United States, exposing over 1.2 million workers to metalworking fluid mists (Beattie and Strohm, 1994; NIOSH, 1977). Over the last forty years, epidemiological studies have associated mist exposures with several adverse health effects. To protect workers, ACGIH recommended a TLV of 5 mg/m^3 of "respirable particles" in 1966, and OSHA adopted the TLV as the PEL in 1970. Since then, the installation of machine enclosures, local exhaust ventilation, and mist collectors has decreased the ambient concentrations of metalworking fluid mists in the workplace (Hallock *et al.*, 1994; Woskie *et al.*, 1994a). Due to the large number of workers exposed, many epidemiological studies have been conducted in an attempt to understand the exposure routes, and potential carcinogenic and non-carcinogenic health effects of metalworking fluids.

Dermal contact is one exposure route for metalworking fluid mist (Bennett and Bennett, 1987). Dermal exposure to metalworking fluid mists is associated with both benign and malignant skin conditions. Contact dermatitis of the hands and forearms due to exposure to soluble and synthetic fluid mists is the most prevalent health problem affecting metal machining workers (De Boer *et al.*, 1989a; De Boer *et al.*, 1989b; Mackerer, 1989). In addition, excessive incidences of skin and scrotal cancer were discovered in workers who were exposed to straight oil mists (Jarvholm *et al.*, 1985; Jarvholm and Lavenius, 1987). The carcinogenicity of straight oil is caused by the polycyclic aromatic hydrocarbons that naturally occur in the straight oil. However, improvements in the straight oil production process have decreased in the polycyclic aromatic hydrocarbon concentration. Therefore, incidences of skin cancer should decrease, unless the chemicals added to the straight oil are carcinogenic (Jarvholm and Easton, 1990; McKee and O'Connor, 1996).

The other metalworking fluid exposure route is inhalation. Inhaled metalworking fluid mist drops in the thoracic size range (mass median diameter of 10.0 μm) are deposited in the tracheobronchial region of the respiratory tract, and respirable oil mist drops (mass median diameter of 4.0 μm) are transported to the alveolar region of the lungs (Vincent, 1995). The inhalation of metalworking fluid mists by humans is associated with non-malignant respiratory effects and a variety of cancers, but not lung cancer (Wagner *et al.*, 1964; Decoufle, 1978).

All three types of metalworking fluids are capable of inducing respiratory problems at exposure concentrations less than 5 mg/m^3 (Robertson *et al.*, 1988). Metalworking fluids are the second most common cause of occupational asthma, and the risk of asthma is elevated at concentrations less than the OSHA PEL of 5 mg/m^3 (Ameille *et al.*, 1995). The asthma manifests as an acute cross-shift decrease in lung function and chronic bronchitis (Kennedy *et al.*, 1989; Ameille *et al.*, 1995; Robins *et al.*, 1995).

Several recent studies have demonstrated a possible increased incidence of many gastrointestinal cancers in metal machining workers after prolonged exposure to mists of all three types of metalworking fluids. Gastrointestinal exposures to metalworking fluid mists result from the transport of large drops from the nasopharyngeal region and thoracic size drops captured by mucoucilliary ladder to the pharynx where the drops are swallowed. For instance, Park *et al.* (1988 and 1996) and Silverstein *et al.* (1988) suggested a positive association between synthetic fluid or soluble oil used in a grinding operation and stomach cancer. Another study indicated an increased risk of bladder cancer in metal machining workers, but did not specify the type of metalworking fluid associated with the cancer (Silverman *et al.*, 1989). Furthermore, rectal and laryngeal cancers are attributed to straight oils, and synthetic fluids are linked to pancreatic cancer (Park and Mirer, 1988; Tolbert et al., 1992; Eisen *et al.*, 1992; Eisen *et al.*, 1994).

In response to these potential health effects, specifically non-malignant respiratory effects, NIOSH (1998) has recommended reducing the PEL for metalworking fluid mist to 0.4 mg/m^3 for thoracic particulate mass, or 0.5 mg/m^3 for total particulate mass. The proposed PEL is a time-weighted average for up to 10 hr/day during a 40 hr/week schedule. In addition, ACGIH (1998) has decreased the TLV to 0.005 mg/m^3 for straight oil containing fifteen carcinogenic polycyclic aromatic hydrocarbons.

D. Mist Control Techniques

Machine enclosures, local exhaust ventilation, and mist collectors are used either separately or in combination to reduce mist concentrations in industrial facilities. Fully or partially enclosing the point of mist generation to provide a physical barrier between the worker and the mist is one method for reducing exposure levels. Placing the entire machine in a sealed chamber is another option that is commonly used for automated machining operations. Local exhaust ventilation can be used with or without a machine enclosure to minimize ambient mist concentrations. Frequently, the mist captured by the ventilation system is conveyed to a mist collector before the air is re-circulated within the plant. The mist also may be discharged to the outside atmosphere as part of the building ventilation system. Types of mist collectors frequently used include filtration or electrostatic precipitation devices. A fully enclosed machine vented to a mist collector equipped with a HEPA or 95% DOP filter should remove most of the mist (Leith *et al.*, 1996). However, some facilities may be hesitant to invest in expensive control equipment to reduce mist concentrations to the recommended PEL.

E. Previous Research

Chan *et al.* (1990) first investigated the size distribution of mist generated in industrial facilities. They found the mist size distribution to be polydisperse with aerodynamic diameters larger than 8 μm and smaller than 1 μm. The large particles were formed by the application of metalworking fluid to the machine; whereas the machining process produced the fine aerosol. Chan *et al.* (1990) also concluded that a metalworking fluid with a greater oil concentration increased the size of the particles generated.

In another study, Woskie *et al.* (1994b) determined the parameters affecting the aerodynamic diameter of mist drops generated in industrial machining plants. The mist was log-normally distributed with mass median diameters between 5 and 8 μm and geometric standard deviations between 2.4 and 3. The machine type, metalworking fluid type, indoor humidity, and outdoor temperature influenced the mass concentration of drops larger than 9.8

μm. For drops smaller than 3.5 μm, the facility, machine type, metalworking fluid type, indoor humidity, and degree of enclosure influenced the mist concentration.

Finally, Smolenski *et al.* (1996) assessed whether altering a metalworking fluid's physical properties would influence the size distribution of a mist generated with a nebulizer. Increasing the elongational viscosity of straight oil by adding polyisobutylene, a high molecular weight polymer, increased the mass median diameter of the mist drops 20% to 200%, depending on the polyisobutylene concentration.

F. Significance of Research

Because Chan *et al.* (1990) and Woskie *et al.* (1994b) collected their data in industrial facilities, they were not able to control various machining and fluid parameters to determine their effect on the mist generation rate and size distribution. However, Woskie *et al.* (1994b) did suggest that the type of material being machined, cutting tool type, and cutting characteristics influenced the mist concentration and size distribution. In addition, the mist generation rates and size distributions from each formation mechanism were not examined individually.

If the mist concentration in industrial environments is to be decreased through changes in the machining process, the effect of specific machining and fluid parameters on the generation rate and size distribution of a mist must be assessed in a controlled environment. A thorough understanding of the mist formation mechanisms may provide insight into methods to reduce economically the ambient oil mist concentrations through pollution prevention.

This research will broaden the scope of the research performed by other researchers, as discussed above. Woskie *et al.* (1994b), Chan *et al.* (1990), and Smolenski *et al.* (1996) investigated the effect of individual parameters or small groups of parameters on mist formation. This research will empirically and theoretically explore the importance and relationships between all fluid and machining parameters that may affect mist formation. In addition, this research is the first attempt at quantitatively determining the contribution of each formation mechanism to the overall mist size distribution.

II. MIST GENERATION

A. Abstract

Use of metalworking fluids during machining results in a mist that is associated with adverse health effects. Experiments conducted on a small lathe quantified the amount of mist generated by evaporation/condensation, centrifugal force, and impaction. Evaporation/condensation was the most important mechanism, followed by centrifugal force, then impaction. For evaporation/condensation, rotational speed and cut depth determined the amount of heat generated during machining, whereas fluid flow determined the amount of heat transferred to the liquid. The flow-rotational speed interaction influenced mist generation by centrifugal force, whereas mist generation by impaction was determined only by fluid flow.

B. Introduction

Metalworking fluids are used frequently during metal machining to increase production rates and prolong tool life. The power consumed during machining is converted to heat that is absorbed by the metal chips, tool, and workpiece (Leep, 1994). The primary function of a metalworking fluid is to cool the cutting tool and workpiece during machining. Flooding the machining area with metalworking fluid cools the tool and flushes chips away from the machining site, thereby prolonging tool life and allowing faster cutting speeds. The metalworking fluid also reduces the friction between the tool and the workpiece, thus increasing tool life and improving the surface finish on the workpiece (Leep, 1994).

During machining, a mist of metalworking fluid is generated. Epidemiological studies have associated mist exposures with several adverse health effects in the 1.2 million metal machining workers in the United States (NIOSH, 1977). Contact dermatitis and an acute cross-shift decrease in lung function are the most prevalent health effects associated with metalworking fluid mists (Jarvholm *et al.*, 1985, Robins *et al.*, 1995). Long term exposures to these mists may be associated with cancer (Park *et al.*, 1988, Tolbert *et al.*, 1992, Silverstein *et al.*, 1988). In response to these potential health effects, NIOSH (1998) recommended setting the permissable exposure limit for metalworking fluid mist at 0.5 mg/m^2.

Achieving the proposed standard with current control practices may be difficult and expensive. Machine enclosures, local exhaust ventilation, and mist collectors are used either separately or in combination to reduce mist concentrations in industrial facilities. A fully-enclosed machine vented to a mist collector equipped with a HEPA or 95% DOP filter should remove most of the mist (Leith *et al.*, 1996). However, some facilities may be hesitant to invest in expensive control equipment.

A more basic means for minimizing mist concentrations is to prevent mist formation. An exposure assessment study by Woskie *et al.* (1994) concluded that the type of metalworking fluid, fluid application rate, and type of machining operation were related to the mist generation rate. At present, published research concerning mist formation during metal machining is limited to that study, and the formation mechanisms are poorly understood.

Potential mist formation mechanisms include impaction, centrifugal force, and evaporation/condensation. High fluid application velocities and pressures may cause the fluid to disintegrate into droplets upon impaction with the tool or workpiece. The number of drops generated depends on the number, size, and amplitude of the surface disturbances on the fluid jet (Bhunia and Lienhard, 1994). The spinning workpiece or tool also may generate mist when the centrifugal force acting on the metalworking fluid exceeds the surface tension force holding the fluid on the workpiece. This process is similar to aerosol generation with a spinning disc generator (Chen, 1992). By equating the surface tension force with the centrifugal force, droplet size can be calculated from:

$$d = \left(\frac{3\,\sigma\, D}{v^2\, \rho} \right)^{0.5} , \tag{2.1}$$

where d is the droplet diameter, D is the cylinder diameter, v is the tangential velocity, σ is the surface tension, and ρ is the fluid density. Condensation of vapor generated by the machining process is the third mist formation mechanism. Heat generated during machining raises the temperature of the tool and chip to more than 200 °C (Childs *et al.*, 1988). A properly operating cooling system transfers this heat to the metalworking fluid. If the metalworking fluid absorbs enough heat, the volatile components may evaporate and then condense upon cooling to form a mist. Shear forces caused by the cutting action do not generate mist because the high contact pressure between the tool, chip, and workpiece prevents the fluid from penetrating the contact area (Childs *et al.*, 1988).

This research characterized the mist formation process by quantifying the mist generated by each formation mechanism and identifying the parameters affecting each. The parameters investigated included machining variables and metalworking fluid properties.

C. Apparatus

As shown in Fig. 2.1, mist was generated on a 2.5-hp lathe (Sears-Roebuck, Chicago, IL) equipped with a carbide steel tool (MSC Industrial Supply, Plainview, NY). A transparent, acrylic housing surrounding the lathe trapped the mist. The relative humidity and temperature within the housing were monitored with a thermo-hygrometer (Fisher Scientific, Pittsburgh, PA).

An Aerosizer LD (Amherst Process Instruments Inc., Hadley, MA) measured the mist size distribution and number concentration by withdrawing mist at 2.5 Lpm from a sampling port on the rear of the housing. The measured concentration and size distribution were converted to the actual number concentration and size distribution via an empirical relationship based on drop size and Aerosizer voltage (Thornburg et al., 1999).

To prevent the mist concentration from exceeding the maximum detection level of the Aerosizer LD, a dilution chamber (not shown in Fig. 2.1) was placed between the housing and the Aerosizer LD. The dilution chamber consisted of a fan to mix the mist uniformly, a filtration system to remove excess mist, and a sample port leading to the Aerosizer LD. Tests showed the dilution chamber could decrease the mist concentration by a factor of 70 while not significantly altering the mist size distribution.

Mist mass concentrations were measured gravimetrically. Two polytetrafluoroethylene (PTFE) filters (Omega Specialty Instruments, Chelmsford, MA) collected mist withdrawn at 1.2 Lpm from sample ports on the housing. Activated carbon tubes (SKC Inc., Eighty-Four, PA) placed behind the filters collected vapor samples. The filters were weighed on an MT5 analytical balance (Mettler-Toledo, Greinfensee,

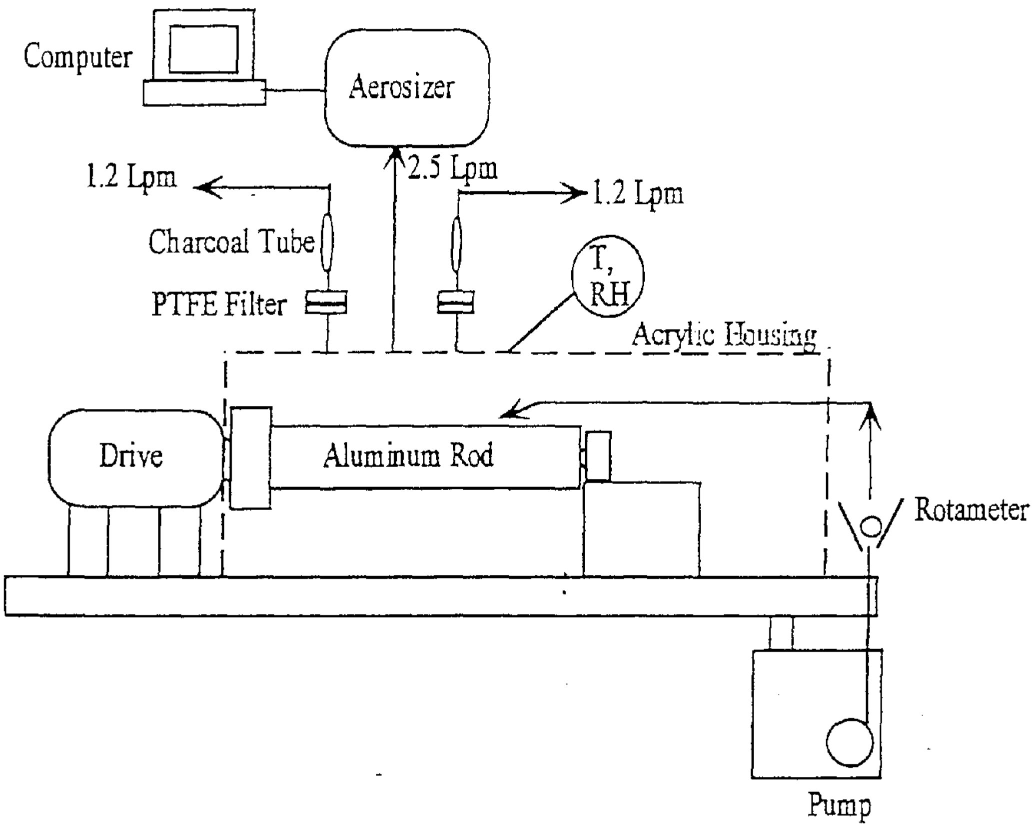

Figure 2.1: Lathe and sampling equipment used during experiments.

Switzerland). Evaporation of mist from the filters did not affect measured concentrations because the air was saturated with organic vapors.

The chemical compositions of the mist and vapor were determined using a GC/MS technique. The filters were placed in glass jars containing carbon disulfide and sonicated for thirty minutes to desorb the mist. The vapor from the activated carbon tubes was extracted with carbon disulfide according to the method described by NIOSH (1975). The mist and vapor samples were analyzed by gas chromatography/mass spectrometry using the method developed by Cooper *et al.* (1996).

The amperage consumed by the lathe was monitored with an ammeter (A.W. Sperry Instruments, Inc., Hauppauge, NY). The amperage applied to the tool, or cutting amperage, was calculated by subtracting the amperage necessary to operate the lathe without machining from the total amperage measured during a machining experiment. The cutting power was calculated by multiplying the cutting amperage by the voltage supplied to the lathe.

Metalworking fluid was applied directly to the cutting surface by high and low pressure Teel pumps, Models 2P406 and 2P400 (W.W. Grainger, Inc., Durham, NC). The applied metalworking fluid was collected in a pan below the lathe, passed through a filter to remove the chips, drained into a sump, and re-used.

Soluble and mineral oil were investigated in this study; their chemical and physical properties are listed in Table 2.1. For all experiments, the soluble oil was an 8% solution of Kleen Kut 6222 (D.A. Stuart Co., Warrenville, IL) in distilled water. An industrial fluid refractometer was used to monitor the soluble oil concentration (Leica AG, Solms, Germany). The surface tension of the soluble oil was decreased by adding 0.5% by volume of Tergitol 15-S-2 nonionic surfactant (Union Carbide Co., Danbury, CT). A Surface Tensiomat 21

Table 2.1: Chemical and physical properties of mineral and soluble oil.

Property	Mineral Oil	Soluble Oil
Viscosity (cp)	Low: ~2.1	Low: ~1.5
	High: ~11.8	High: ~1.9
Surface Tension (dynes/cm)	Low: ~22	Low: ~26
	High: ~26	High: ~29
Boiling Point (°C)	225 to 220[A]	~100[B]
Specific Heat (J/g-K)	~2.2[A]	~4.2[B]
Heat of Vaporization (J/g)	~250[A]	~2400[B]

[A]Values depend on individual components of mineral oil

[B]Soluble oil contains >92% water so the values of water were used as approximations

(Fisher Scientific, Pittsburgh, PA) measured the fluid surface tension. The soluble oil viscosity was increased by adding 1% by volume of Tergitol 15-S-7 nonionic surfactant (Union Carbide Co., Danbury, CT), and was measured with a viscometer (Haake Mess-Technik, Germany). The low and high viscosity mineral oils used were Fuchs 7911 and Fuchs 1922 (Fuchs Lubricants Co., Harvey, IL), respectively. More than 90%, by mass, of the Fuchs 7911 consisted of n-alkanes ranging from tridecane to nonadecane. The mass fraction of these n-alkanes in Fuchs 1922 was less than 9%, with the remaining 91% consisting of higher molecular weight n-alkanes. Adding 1% by volume of n-hexanes reduced the surface tension of the mineral oils without altering the viscosity. The density of the soluble and mineral oils was measured with a Mettler AE200 balance (Mettler-Toledo, Greinfensee, Switzerland) and a graduated cylinder.

D. Experiments

Three sets of experiments investigated mist generation by impaction, centrifugal force, and evaporation/condensation. The parameters and experimental conditions for each set of experiments are discussed below.

1. Impaction

The contribution of impaction to mist generation was investigated by applying the metalworking fluid to the cutting tool without rotating or machining a 7.6 cm diameter aluminum rod (Alcoa, Pittsburgh, PA). The tool was placed 0.002 cm from the rod. Mist number concentration was measured with the Aerosizer LD connected to the housing. The average of three replicates equaled the mist generated by impaction. Samples were collected for four minutes at 2.5 Lpm. Filter and vapor samples were not collected during these tests.

The metalworking fluid type and flow rate were varied during the experiments (Table 2.2). Each condition was tested three times, yielding 9 experiments for each metalworking fluid.

2. Centrifugal Force

Identical combinations of fluid type and flow were investigated while the aluminum rod rotated at four rotational speeds to investigate the influence of centrifugal force on mist generation (Table 2.2). The same sampling procedure as described above was used. Three replicate tests of each combination of parameters were conducted, yielding 26 experiments for each metalworking fluid. Differences in average mist number concentration between the impaction and centrifugal force experiments were attributed to the centrifugal force mechanism.

3. Machining

Aluminum rods were machined on the lathe to quantify mist generation from evaporation/condensation of mineral and soluble oil. The Aerosizer LD measured the total mist number concentration. The contribution of evaporation/condensation to the number concentration equaled the total concentration minus the average concentrations generated by impaction and centrifugal force. The mist mass concentration was measured gravimetrically with PTFE filters. For all mineral oil experiments, the dilution chamber was used and vapor samples were collected with activated carbon tubes. Soluble oil vapor concentrations were not high enough to be detected by the GC-MS.

The parameters investigated during the machining experiments for soluble and mineral oil are listed in Table 2.3. The metal hardness, tool rake angle, tool feed rate, rotational speed, and depth of cut comprised the operating characteristics of the lathe. The rake angle

Table 2.2: Parameters investigated during impaction and centrifugal force tests.

Soluble Oil, Low Viscosity		Mineral Oil, Low Viscosity	
Flow (ml/sec)	Rev/s[A]	Flow (ml/sec)	Rev/s[A]
2.4	8.2	2.4	8.2
6.6	12.4	6.6	12.4
10	21.2	10	21.2
	25.5		25.5

[A]Investigated only during centrifugal force tests

Table 2.3: Machining experimental conditions for mineral and soluble oil.

Variable	Low Level	High Level
Metal Type	Aluminum 6061	Aluminum 2024
Tool Rake Angle	0 degrees	15 degrees
Machining Rate	0.011 cm/rev	0.016 cm/rev
Rotational Speed	8.2 rev/s	21.2 rev/s
Depth of Cut	0.12 mm	0.51 mm
Viscosity	Low	High
Surface Tension	Low	High
Flow	2.4 ml/sec	10 ml/sec
Fluid Temperature	22 °C	20 °C
Tramp Oil Concentration	0%	5%

was the only tool parameter determining cutting power, so all other tool parameters remained constant (Oberg *et al.*, 1984). The fluid viscosity, surface tension, flow, temperature, and tramp oil contamination represented the metalworking fluid characteristics. Tramp oil contamination was simulated by adding 0.5% by volume of Heavy Gear Oil (William H. Harvey Co., Omaha, NE) to the metalworking fluid. Addition of tramp oil did not measurably affect the surface tension or viscosity of the metalworking fluids.

A two level, twelve run Plackett-Burman plan initially identified which of the eleven parameters caused variations in the mist generation rate (Diamond, 1981). These parameters were examined in more detail using an additional 2^2 factorial design.

E. Results

The general linear models procedure in SAS (SAS Institute Inc., Cary, NC) was used to analyze the data. All statistical tests were performed at the 95% confidence level. For the impaction and centrifugal force data, analysis of variance in conjunction with Tukey tests identified the parameters influencing mist generation. Transforming the machining mist generation data by the reciprocal square root stabilized the residuals. Ordinary least squares of the transformed data identified the parameters affecting mist generation during the machining experiments.

For impaction, increasing fluid flow increased the mist number concentration generated (p-value = 0.0001); metalworking fluid type (p-value = 0.77) had no measurable effect.

The mist number concentration generated by centrifugal force equaled the total generated by the spinning workpiece minus the contribution from impaction. Mist number concentration was influenced by the rotational speed (p-value = 0.0005), fluid flow (p-value = 0.0009), and fluid flow-rotational speed interaction term (p-value = 0.0001), while metalworking fluid type (p-value = 0.22) had no measurable effect. A simultaneous increase in fluid flow and rotational speed consistently increased the mist number concentration at all experimental conditions. Increasing rotational speed alone affected mist generation only at fluid flows greater than 10 ml/sec.

The mist number concentration generated by evaporation/condensation equaled the total generation during machining minus the contributions from impaction and centrifugal force. Only rotational speed, depth of cut, and fluid flow measurably influenced mineral and soluble oil mist generation during machining (Table 2.4). For both fluids, increasing the rotational speed and depth of cut generated more mist, whereas increasing the fluid flow decreased mist generation (Fig. 2.2). None of the second or third order interactions were statistically significant for either fluid.

Both soluble and mineral oil generated measurable quantities of vapor. During machining with soluble oil, the relative humidity in the chamber increased from ambient levels (20%-50%) to more than 90%. The mineral oil vapor concentration was positively influenced by the rotational speed (p-value = 0.0008) and depth of cut (p-value = 0.002). The mineral oil viscosity did not affect mist and vapor generation.

The mineral oil mist and vapor consisted of n-alkanes between tridecane and nonadecane, and the compositions were independent of viscosity. For low viscosity mineral oil, the mass fraction of the n-alkanes comprising the mist and vapor are compared to the bulk fluid in Fig. 2.3.

Table 2.4: Parameters influencing evaporation/condensation of mineral and soluble oil.

Mineral Oil		Soluble Oil	
Parameter	p-value	Parameter	p-value
Cut Depth	0.0002	RPM	0.0008
Flow	0.0056	Flow	0.0022
RPM	0.0077	Cut Depth	0.0027

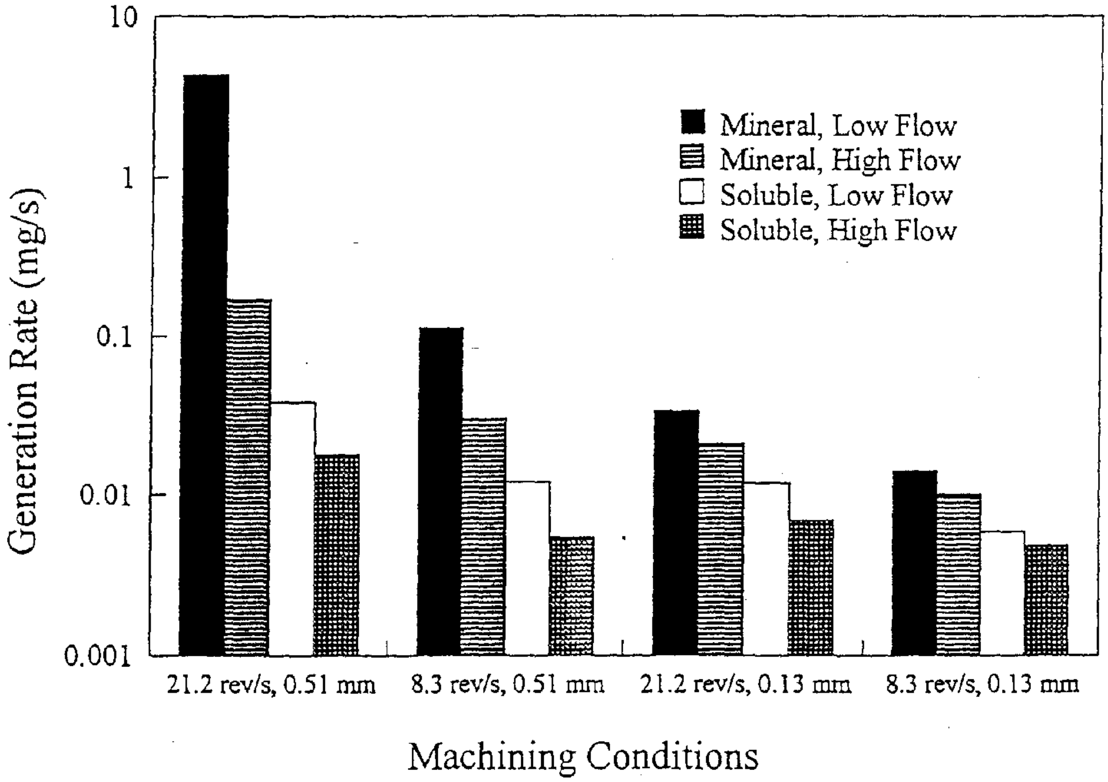

Figure 2.2: Mist generation rate for different combinations of rotational speed, cut depth, fluid flow, and metalworking fluid type.

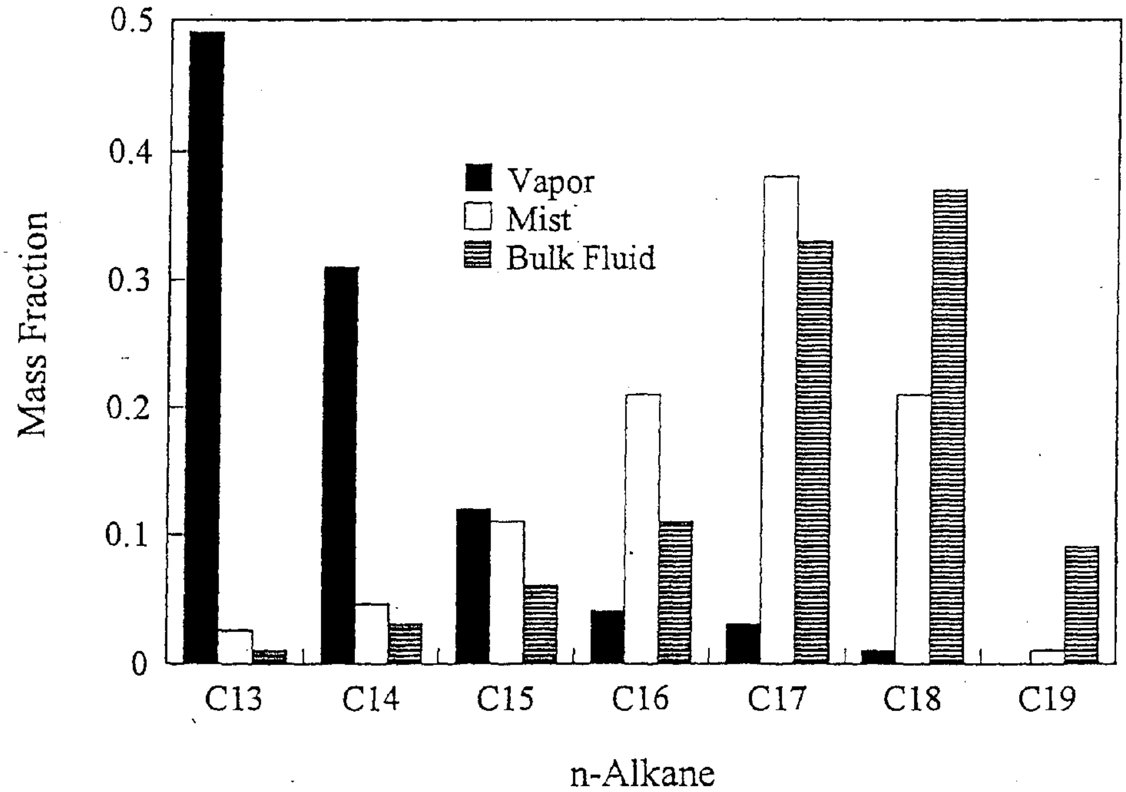

Figure 2.3: Composition of mineral oil bulk fluid, mist, and vapor.

Figure 2.4 shows the contribution of each formation mechanism to the mineral oil mist number concentration as a function of particle size. Fluid flow, rotational speed, and cut depth were 10 ml/sec, 21.2 rev/s, and 0.51 mm, respectively. The impaction and centrifugal force curves are the averages of three replicate tests. Figure 2.5 is an analogous plot for soluble oil at the same experimental conditions. Similar data for both metalworking fluids were obtained for other experimental conditions but are not shown.

Figures 2.4 and 2.5 show that impaction produced the fewest number of particles, and most were smaller than 8 μm. Centrifugal force generated most of the particles larger than 8 μm, and about the same number of particles smaller than 8 μm as impaction. Machining generated 1,000 to 10,000 more particles smaller than 8 μm than did either impaction or centrifugal force.

Figure 2.2 indicates mineral oil produced more mist than soluble oil under similar operating conditions. Within our ability to detect differences, the type of metalworking fluid did not affect the cutting power (Table 2.5). Therefore, the higher mineral oil mist concentrations were not caused by the production of additional heat during machining. The cutting power was positively correlated with rotational speed (p-value = 0.0001), and cut depth (p-value = 0.0001). The rotational speed-cut depth interaction term (p-value = 0.0006) reinforced their effect on the cutting power.

F. Discussion

Impaction was a secondary source of mist drops. However, mist generation by impaction increased proportionally with fluid flow. In industrial facilities, impaction should be a more important source of mist because the fluid flow is much greater.

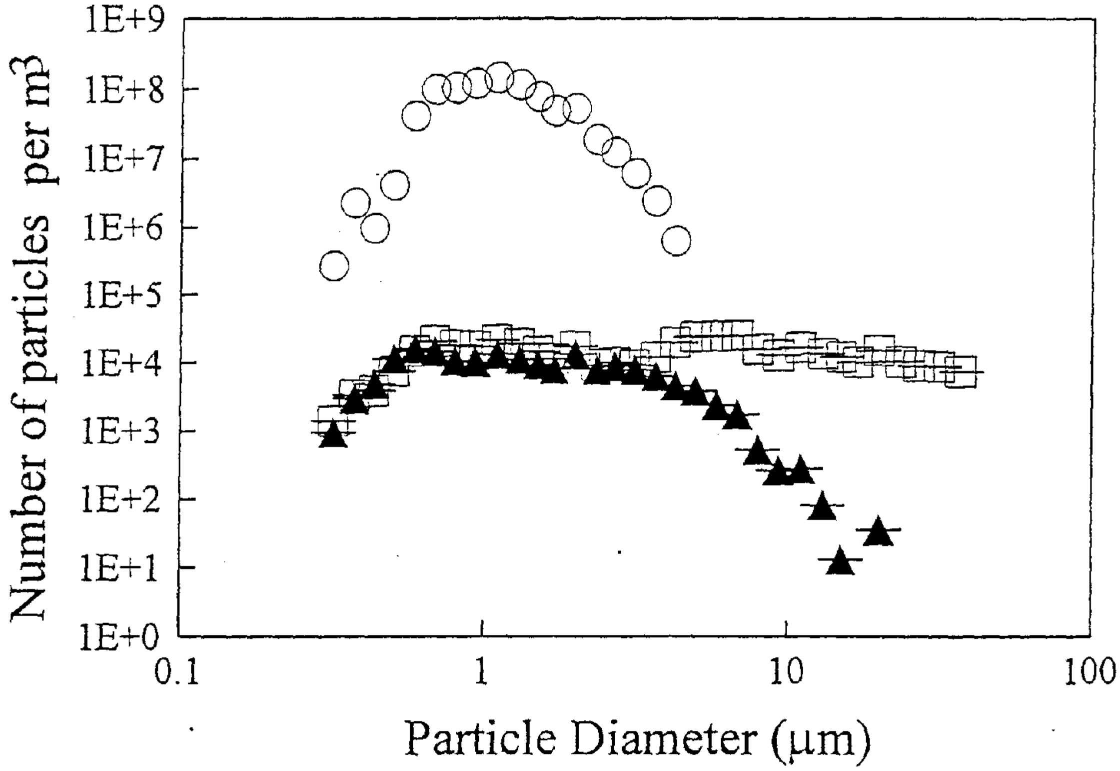

Figure 2.4: Mineral oil number concentration generated by evaporation/condensation (○), centrifugal force (□), and impaction (▲). Rotational speed was 21.2 rev/s, cut depth was 0.51 mm, and flow was 10 ml/s.

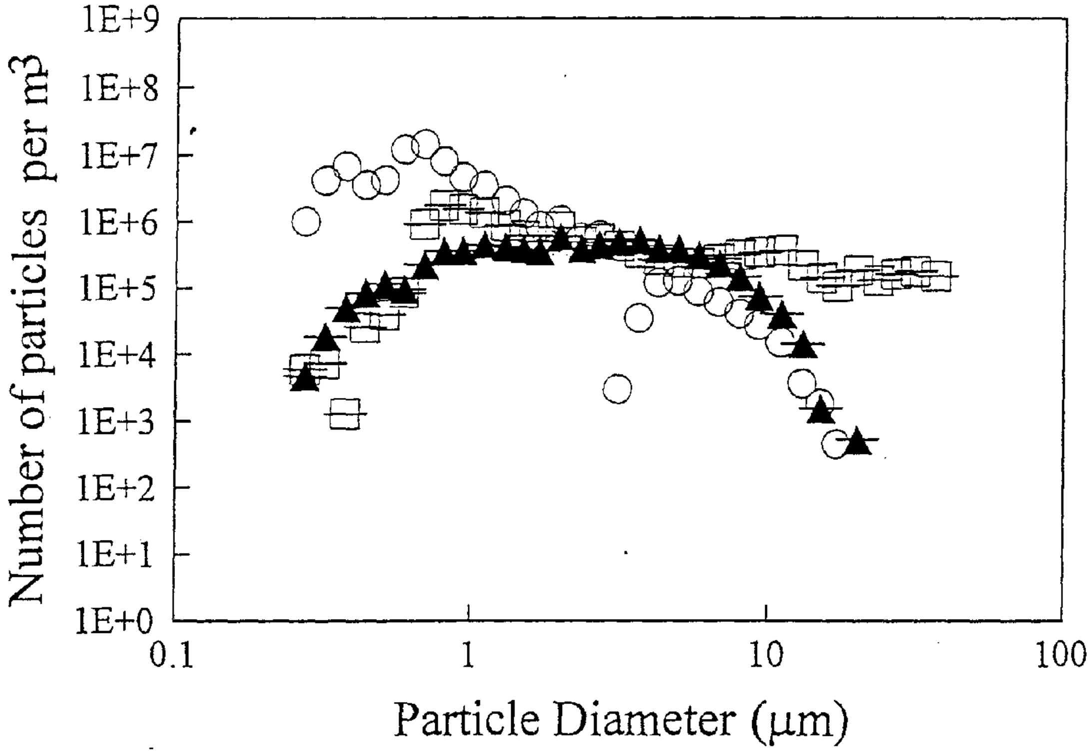

Figure 2.5: Soluble oil number concentration generated by evaporation/condensation (○), centrifugal force (□), and impaction (▲). Rotational speed was 21.2 rev/s, cut depth was 0.51 mm, and flow was 10 ml/s.

Table 2.5: Differences in average cutting power consumed while machining with mineral and soluble oil at different conditions.

Machining Conditions		Average Cutting Power (W)		
Rotational Speed	Depth of Cut	Mineral Oil	Soluble Oil	p-value
500	0.005	22.0 ± 27.2	24.8 ± 17.8	0.67
500	0.02	51.7 ± 54.7	71.5 ± 26.2	0.52
1270	0.005	56.4 ± 29.6	79.8 ± 26.5	0.25
1270	0.02	281 ± 52.5	298 ± 122	0.80

From Eq. 2.1, the drop size generated by the workpiece rotating at 21.2 and 8.2 rev/s was 500 and 1200 µm, respectively. Particles this large settled gravitationally or formed smaller drops upon colliding with the housing wall before being sampled by the Aerosizer LD. The collision of the drops with the housing wall probably generated secondary 8 to 50 µm particles that were measured by the Aerosizer LD. The number of drops generated by impaction with the wall depended on the physical and kinematic properties of the fluid and the surface conditions of the wall (Mundo *et al.*, 1996). More secondary drops were created at higher rotational speeds because the higher tangential velocity transported more drops to the wall and decreased the stability of the drops.

Evaporation and subsequent condensation of the fluid during machining was the major mist formation mechanism. Increasing the rotational speed and cut depth required more cutting power, which increased the amount of heat and mist generated. Woskie *et al.* (1994) found that mist generation was affected by the machine type-fluid interaction, which could have been related to the rotational speed and cut depth of the machine. Although rotational speed and cut depth were not investigated in that study, Woskie *et al.* (1994) suggested that a lower cutting speed would generate less mist, as evidenced by Fig. 2.2. Increasing the fluid flow decreased mist generation by decreasing the amount of heat absorbed per unit mass of fluid.

Rotational speed, cut depth, and fluid flow can be combined into a dimensionless mist generation number, M, defined as the metal removal rate, Q_m, divided by the fluid flow, Q_f,

$$M = \frac{Q_m}{Q_f}. \tag{2.2}$$

In Eq. 2.2, the metal removal rate equals the product of the surface area of metal removed per second and the cut depth, C:

$$Q_m = \Pi D \omega F C \,, \tag{2.3}$$

where D is the diameter of the rod, ω is the rotational speed, and F is the machining rate.

As shown in Fig. 2.6, M is proportional to the mist generation rate, G. Therefore, an increase in Q_m or a decrease in Q_f will cause an increase in G. Figure 2.6 also shows that mineral oil produced more mist than soluble oil for a constant value of M. The slopes of the regression lines in Fig. 2.6 probably depended on the heat absorption potential of the particular metalworking fluid.

Mineral oil produced more mist than soluble oil because of differences in the heat absorption potential and saturated vapor pressure of the fluids. The heat absorption potential is the heat per unit mass necessary to evaporate the fluid and equals the heat capacity of the fluid, H_{cap}, plus the heat of vaporization, H_{vap}. The heat capacity of the fluid is related to the specific heat, C_p, boiling point, T_{BP}, and initial temperature, T_o, by:

$$H_{cap} = C_p (T_{BP} - T_o) \,. \tag{2.4}$$

Values for C_p and T_{BP} were taken from Perry and Green (1997).

Because the soluble oil contained 92% water, the C_p and T_{BP} of water were used in Eq. 2.4. Therefore, heat capacity for soluble oil was about 200 J/g. The heat capacity of the n-alkanes comprising mineral oil was between 460 and 690 J/g. The heat of vaporization was approximately 250 J/g for each n-alkane and 2400 J/g for the water in soluble oil (Lide, 1997). Therefore, the heat absorption potential of mineral oil was less than 1040 J/g versus 2700 J/g for soluble oil. As a result, more heat was required to evaporate the soluble oil.

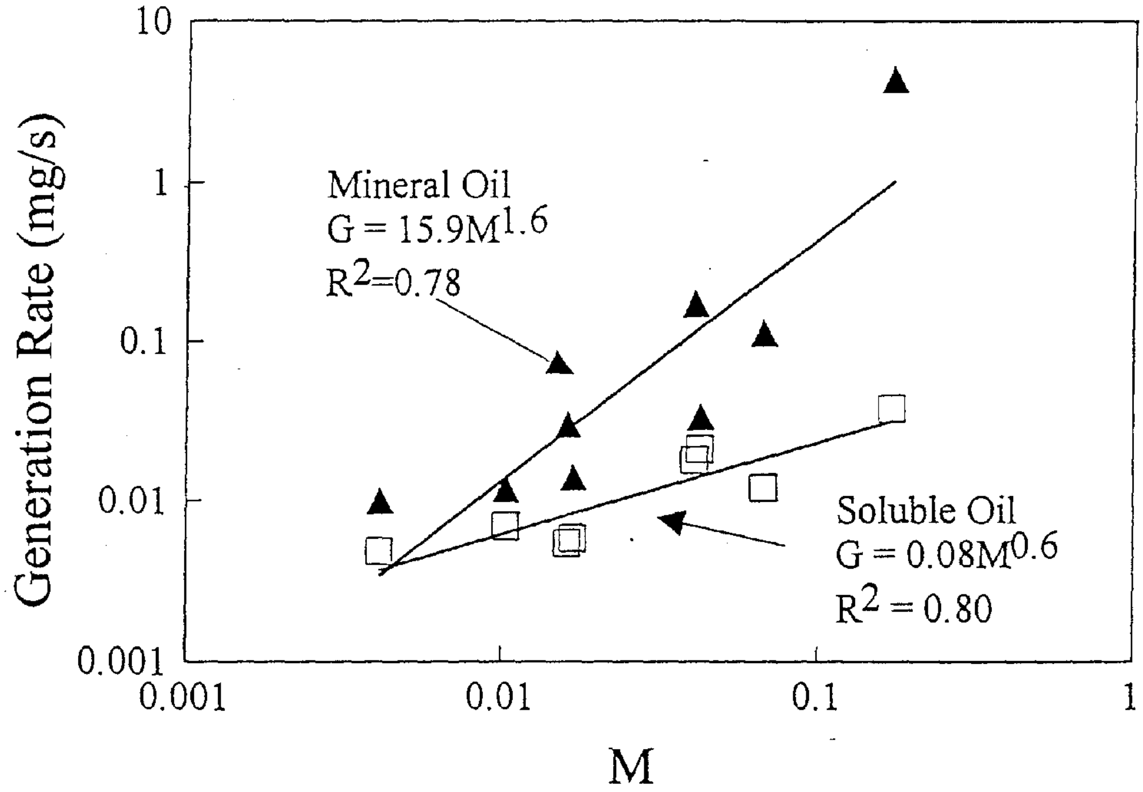

Figure 2.6: Soluble (□) and mineral oil (▲) mist generation rate, G, as a function of the dimensionless mist generation number, M.

The saturated vapor pressure also determined the amount of mineral and soluble oil that condensed and the mass fraction of each n-alkane in the mist and vapor. Saturated vapor pressures for the n-alkanes and water at 22 °C were estimated from Yaws (1994) and Green and Perry (1997), respectively. Heptadecane, octadecane, and nonadecane have vapor pressures less than 10^{-5} kPa and readily condensed. From Fig. 2.2, the mineral oil mist contained more than 20% octadecane and 25% heptadecane, while the combined mass fraction of these compounds in the vapor phase was less than 5%. All the nonadecane that evaporated during machining condensed. However, significant quantities of tridecane and tetradecane did not condense because their saturated vapor pressures were greater than 10^{-2} kPa. Tridecane and tetradecane comprised more than 70% of the vapor and less than 10% of the mist. Similarly, a high saturated vapor pressure, 2.5 kPa, prevented condensation of the water evaporated from soluble oil. The condensation of the oil phase, probably containing n-alkanes like those in mineral oil, was the source of soluble oil mist. Therefore, soluble oil produced less mist than mineral oil because the mass fraction of compounds with "low" saturated vapor pressures that condensed was higher in mineral oil.

G. Conclusions

Evaporation and condensation of the metalworking fluid from the heat generated during machining was the major mist formation mechanism, followed by centrifugal force, then impaction. Mineral oil generated more mist than soluble oil under the same machining conditions because the components of mineral oil evaporated more easily and have lower saturated vapor pressures.

During these experiments the fluid flow, depth of cut, and rotational speed were much lower than those used in an industrial process. Higher fluid flows in industry will improve the cooling effect of the fluid, possibly offsetting additional mist generation by higher rotational speeds or deeper cuts. In addition, larger flows will increase mist generation by impaction, and higher rotational speeds will produce more particles via centrifugal force.

Finally, we were not concerned with the quality of the surface finish or tool wear while investigating the mist formation mechanisms. Both of these factors help determine the type and amount of metalworking fluid used. Plant management may not want to change metalworking fluids or increase fluid flow because of potential detrimental effects to the surface finish or decreased tool life.

III. MIST SIZE DISTRIBUTION

A. Abstract

Mist generated by machining processes is formed by three mechanisms: impaction, centrifugal force, and evaporation/condensation. This study characterized the size distribution of soluble and mineral oil mists that resulted from these formation mechanisms. Salient parameters influencing the particle size distributions also were identified. Variables investigated included metalworking fluid and machining characteristics. The size distribution of the mist generated on a small lathe by each mechanism was measured using an Aerosizer LD. For impaction, only the mineral oil viscosity influenced the mass median diameter of the mist. No parameter affected the geometric standard deviation. High viscosity mineral oil had a mass median diameter of 6.1 μm and a geometric standard deviation of 2.0. Low viscosity mineral oil had a mass median diameter of 21.9 μm and a geometric standard deviation of 2.2. The mass median diameter of the mist generated by centrifugal force depended on the type of metalworking fluid, fluid flow, and rotational speed of the lathe. Mass median diameters for low viscosity mineral oil ranged from 5 to 110 μm. Mass median diameters for soluble oil varied between 40 and 80 μm. The average geometric standard deviation was 2.4, and was not affected by any parameter. The mass median diameter and geometric standard deviation of the mist generated by evaporation/condensation varied with the type of metalworking fluid. The mineral oil and soluble oil mass median diameters were 2.1 μm and 3.2 μm, respectively. No machining or fluid parameter was

important because the mist size distribution depended on the rate of condensation, coagulation processes, and the dynamics of the apparatus. Quantifying and understanding which parameters influence the mist size distribution generated by each formation mechanism may allow industrial hygienists to decrease worker exposure to the smallest mist drops.

B. Introduction

Exposure to metalworking fluid mist generated by metal machining processes is associated with various adverse health effects. Long term exposure to droplets larger than 4 µm may be associated with gastrointestinal cancers (Park *et al.*, 1988; Silverman *et al.*, 1989). Short term exposure to droplets smaller than 4 µm is correlated with an acute cross-shift decrease in lung function, whereas long term exposure may cause chronic bronchitis (Ameille *et al.*, 1995; Kennedy *et al.*, 1989; Robins *et al.*, 1995). Because these potential health effects exist, NIOSH (1998) recommended to reduce the PEL for metalworking fluid mist to 0.4 mg/m^3 for thoracic particulate mass, or 0.5 mg/m^3 for total particulate mass

This study characterized the mist size distribution resulting from the three formation mechanisms: impaction, centrifugal force, and evaporation/condensation. A better understanding of the machining and fluid parameters that affect the mist size distribution may lead to modified machining operations or metalworking fluids that produce larger droplets. Larger droplets are collected more efficiently by mist collectors (Leith *et al.*), do not penetrate as far into the lungs, and settle more quickly by gravity. Therefore, formation of larger drops reduces a workers' exposure to the mist.

Chan *et al.* (1990) first investigated the size distribution of mist generated in industrial facilities. They found the mist size distribution to be polydisperse with aerodynamic diameters larger than 8 μm and smaller than 1 μm. The large drops were formed by the application of metalworking fluid to the machine, whereas the machining process produced the fine aerosol. Chan *et al.* (1990) also concluded that a metalworking fluid with a higher oil concentration increased the size of the drops generated.

In another study, Woskie *et al.* (1994) determined the parameters affecting the aerodynamic diameter of mist droplets generated in industrial machining plants. The mist sampled was log-normally distributed with mass median diameters between 5 and 8 μm and geometric standard deviations between 2.4 and 3. Machine type, metalworking fluid type, indoor humidity, and outdoor temperature influenced the mass concentration of drops larger than 9.8 μm. For drops smaller than 3.5 μm, the facility, machine type, metalworking fluid type, indoor humidity, and degree of enclosure were important.

Because Chan *et al.* (1990) and Woskie *et al.* (1994) collected their data in industrial facilities, they were not able to control various machining and fluid parameters to determine their effect on the mist size distribution. However, Woskie *et al.* (1994) did suggest that the type of material being machined, cutting tool type, and cutting characteristics influenced the mist concentration and size distribution. Further, the mist size distributions from each formation mechanism were not examined individually by those researchers.

In the previous chapter, the amount of mist generated was measured, and the parameters that influenced the mist generated by impaction, centrifugal force, and evaporation/condensation were identified. In this chapter, the mist size distribution generated by each mechanism was measured and the parameters influencing the mist size distribution from each mechanism were identified. These experiments were conducted in a controlled environment where each parameter was varied.

C. Apparatus

The experimental apparatus, shown in Fig. 3.1, was described in Chapter 2 and will be summarized briefly here. Mist was generated on a 2.5-hp lathe (Sears-Roebuck, Chicago, IL) surrounded by a transparent, acrylic housing to trap the mist. The relative humidity and temperature within the housing were monitored with a thermo-hygrometer (Fisher Scientific, Pittsburgh, PA).

An Aerosizer LD (Amherst Process Instruments Inc., Hadley, MA) measured the aerodynamic diameter of mist drops sampled at 2.5 Lpm from a port on the rear of the housing. To prevent the mist concentration from exceeding the maximum detection level of the Aerosizer LD, a dilution chamber could be placed between the housing and the Aerosizer LD.

Metalworking fluid was applied directly to the cutting surface by a chemical pump (W.W. Grainger, Inc., Durham, NC). The applied metalworking fluid was collected in a pan below the lathe, passed through a filter to remove the chips, drained into a sump, and re-used.

Soluble and mineral oil were investigated in this study. The soluble oil used was Kleen Kut 6222 (D.A. Stuart Co., Warrenville, IL). An industrial fluid refractometer (Leica AG, Solms, Germany) was used to monitor the soluble oil concentration before and after each experiment. The surface tension of the soluble oil was reduced by adding 0.5% by volume of Tergitol 15-S-4 nonionic surfactant (Union Carbide Co., Danbury, CT). A Surface Tensiomat 21 (Fisher Scientific, Pittsburgh, PA) measured the surface tension. The

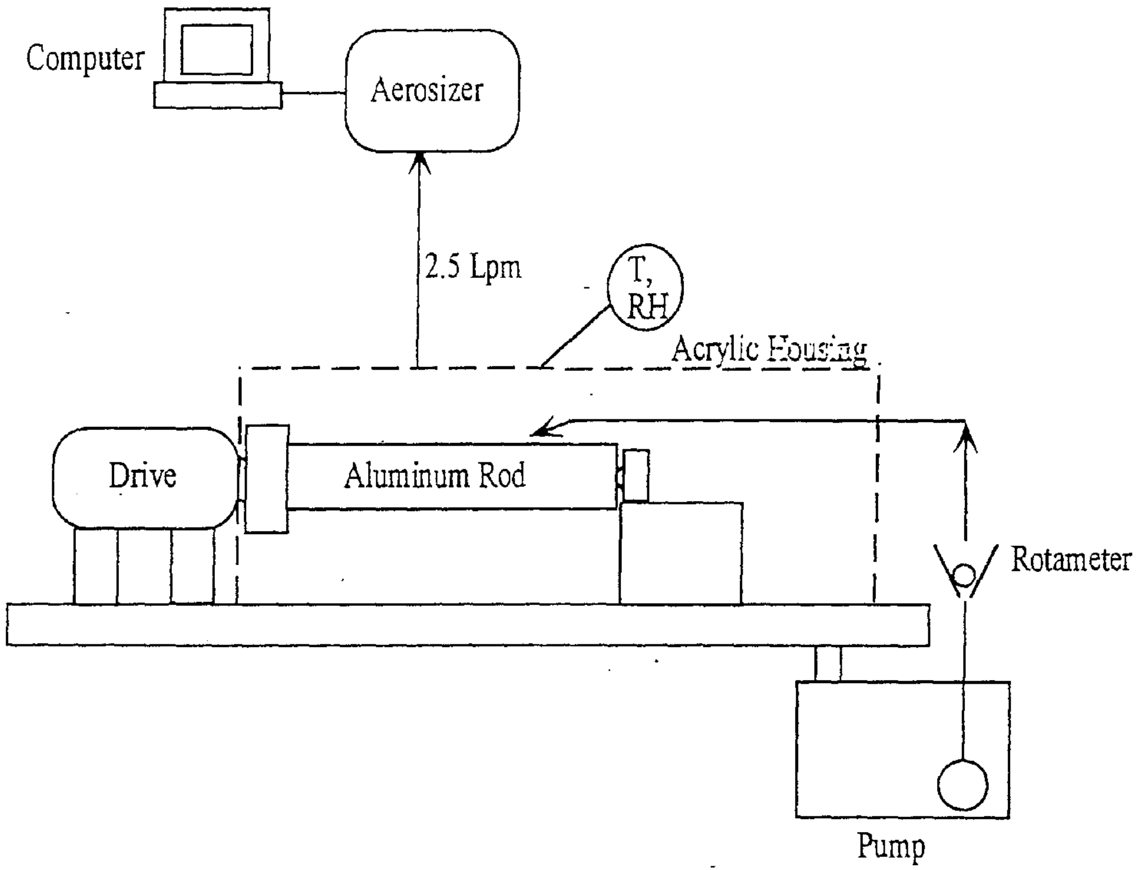

Figure 3.1: Mist generation and sampling equipment used during experiments (dilution chamber not shown).

low and high viscosity mineral oils used were Fuchs 7911 and Fuchs 1922 (Fuchs Lubricants Co., Harvey, IL), respectively. The viscosity of the two metalworking fluids was measured with a viscometer (Haake Mess-Technik, Germany). The density of both metalworking fluids was measured with a Mettler AE200 balance (Mettler-Toledo, Greinfensee, Switzerland) and a graduated cylinder.

D. Experiments

Three sets of experiments investigated mist size distribution generated by impaction, centrifugal force, and evaporation/condensation. The parameters and experimental conditions for each set of experiments are discussed below.

1. Impaction

The size distribution of the mist generated by impaction was investigated by applying the metalworking fluid to the cutting tool without rotating or machining a three-inch diameter aluminum rod (Alcoa, Pittsburgh, PA). The tool was placed 0.003 cm from the rod. The mist size distribution was measured with the Aerosizer LD connected to the housing. Samples were collected for three minutes at 2.5 Lpm.

Soluble oil flow, surface tension, and concentration were investigated individually while the other parameters were held constant at the baseline conditions listed in Table 3.1. Similarly for mineral oil, the flow and viscosity were tested individually. Tests at each experimental condition were conducted three times.

2. Centrifugal Force

The sampling procedure described above was used for the centrifugal force tests, except the aluminum rod rotated at each of four different speeds. For soluble oil, rotational

Table 3.1: Experimental conditions for impaction and centrifugal force experiments.

Parameter	Soluble Oil	Mineral Oil
Flow (ml/s)	4, 6, 8^{A}, 10	4, 6, 8^{A}, 10
Surface Tension (dyne/cm)	26, 29^{A}	26^{A}
Concentration (%)	4, 8^{A}, 12	-
Viscosity (cp)	1.4^{A}	3.1^{A}, 11.8
Rotational Speed (rev/s)	8.3, 13.4, 21.2^{A}, 35.5	8.3, 13.4, 21.2^{A}, 35.5

A: Denotes baseline condition for each oil.

speed was investigated in addition to flow, surface tension, and oil concentration (Table 3.1). Likewise, the effects of rotational speed, flow, and viscosity on the mist size distribution were investigated for mineral oil (Table 3.1). Each parameter was investigated individually while the others remained constant at their baseline setting, and tests at each experimental condition were conducted three times. Once important parameters were identified, additional tests were conducted to clarify the nature of their effect on the mist size distribution.

The drops contributed by the impaction and centrifugal force mechanisms to the total size distribution measured by the Aerosizer LD were assumed to be additive. Therefore, the size distribution generated by impaction at the appropriate condition was subtracted from the total mist size distribution to calculate the size distribution generated by centrifugal force.

3. Evaporation/Condensation

Aluminum rods were machined on the lathe to determine the mist size distribution generated from the evaporation/condensation of mineral and soluble oil. The dilution chamber was used for all mineral oil experiments. Again, the contribution of each mechanism to the total mist size distribution was assumed to be additive. Therefore, the size distribution resulting from evaporation/condensation equaled the total mist size distribution minus the size distribution of the combined impaction and centrifugal force mechanisms at the same flow and rotational speed.

The parameters investigated during the evaporation/condensation experiments are listed in Table 3.2. The metal hardness, tool rake angle, tool feed rate, rotational speed, and depth of cut comprised the operating characteristics of the lathe. Because the rake angle was the only tool parameter that determined cutting power, all other tool parameters remained

Table 3.2: Experimental conditions for machining experiments.

Machining Parameters	*Low Level*	*High Level*
Metal	Aluminum 6061	Aluminum 2024
Rake Angle (degrees)	0^{A}	15
Feed Rate (cm/rev)	0.011	0.016^{A}
Rotational Speed (rev/s)	8.3	21.2^{A}
Cut Depth (cm)	0.013^{A}	0.051
Fluid Parameters	*Low Level*	*High Level*
Flow (ml/s)	4	10^{A}
Temperature (°C)	25^{A}	32
Mineral Oil Viscosity (cp)	3.1^{A}	11.8
Soluble Oil Surface Tension (dyne/cm)	26	29^{A}
Soluble Oil Concentration (% by vol.)	$8\%^{A}$	12%

A: Denotes baseline machining conditions.

constant (Oberg *et al.*, 1984). Fluid type, flow, temperature, viscosity, surface tension, and soluble oil concentration represented the metalworking fluid characteristics.

A two level, eight run Plackett-Burman plan initially investigated the effect of metal hardness, rake angle, feed rate, rotational speed, cut depth, flow, and fluid temperature on the mist size distribution generated by mineral and soluble oil (Diamond, 1981). Potentially significant parameters and their interaction terms were examined in more detail with additional factorial experiments. Soluble oil surface tension and concentration, and mineral oil viscosity remained at their baseline conditions for these experiments.

The effects of soluble oil surface tension, soluble oil concentration, and mineral oil viscosity on the size distribution were investigated individually. All other machining parameters remained at the baseline conditions identified in Table 3.2. Each test for these three parameters was conducted three times.

4. Data Analysis

The size distribution data collected during the three sets of experiments were corrected for errors in the counting efficiency of the Aerosizer LD using an empirical correlation developed by Thornburg *et al.* (1999). Preliminary experiments and other researchers have shown the mist size distribution data were approximately log-normally distributed (Woskie *et al.*, 1994). Therefore, the mass median diameter, MMD, and geometric standard deviation, GSD, were used to characterize the mist size distribution. The MMD and GSD were calculated by fitting a regression line by the least squares method to the size distribution data from each experiment plotted as a cumulative log-probability graph. For each set of experimental conditions, the MMD and GSD from the regressions were averaged together. Differences in the average MMD and GSD were identified using the general linear methods procedure in SAS (SAS Institute, Cary, NC). The data were analyzed at the 95% confidence level.

E. Results

The R^2 value for the regression line fit to the size distribution data was greater than 0.8 for every experiment.

1. Impaction

For the impaction experiments, the average MMD and GSD for the two metalworking fluids are listed in Table 3.3. Only viscosity influenced the mineral oil size distribution, and none of the parameters affected the soluble oil size distribution. There was no important difference in the GSDs of the two metalworking fluids. Note that the soluble oil MMD was approximately the same as the high viscosity mineral oil MMD.

2. Centrifugal Force

Fluid flow and rotational speed influenced the MMD from the soluble and low viscosity mineral oil centrifugal force experiments. Fluid flow was used to determine the fluid application velocity, V_j, and rotational speed was transformed to the tangential velocity of the rotating aluminum rod, V_t. The dimensionless ratio of these velocities, V_j/V_t, is plotted against the average MMD for soluble and low viscosity mineral oil in Fig. 3.2.

The size distribution of the high viscosity mineral oil mist generated by centrifugal force did not vary with fluid flow or rotational speed. The average MMD of the high viscosity mineral oil mist measured by the Aerosizer LD was 4.3 μm ± 0.8 μm. Table 3.4 lists the average GSD for each metalworking fluid. The GSD of the mist for the two metalworking fluids was independent of all parameters.

Table 3.3: Average mass median diameters and geometric standard deviations, with standard error estimates, from impaction experiments.

Fluid Type	# Observations	Average MMD (μm)	Average GSD
Mineral Oil, low viscosity	12	21.9 ± 1.8	2.2 ± 0.1
Mineral Oil, high viscosity	6	6.1 ± 1.5	2.0 ± 0.1
Soluble Oil	21	6.0 ± 0.6	2.1 ± 0.04

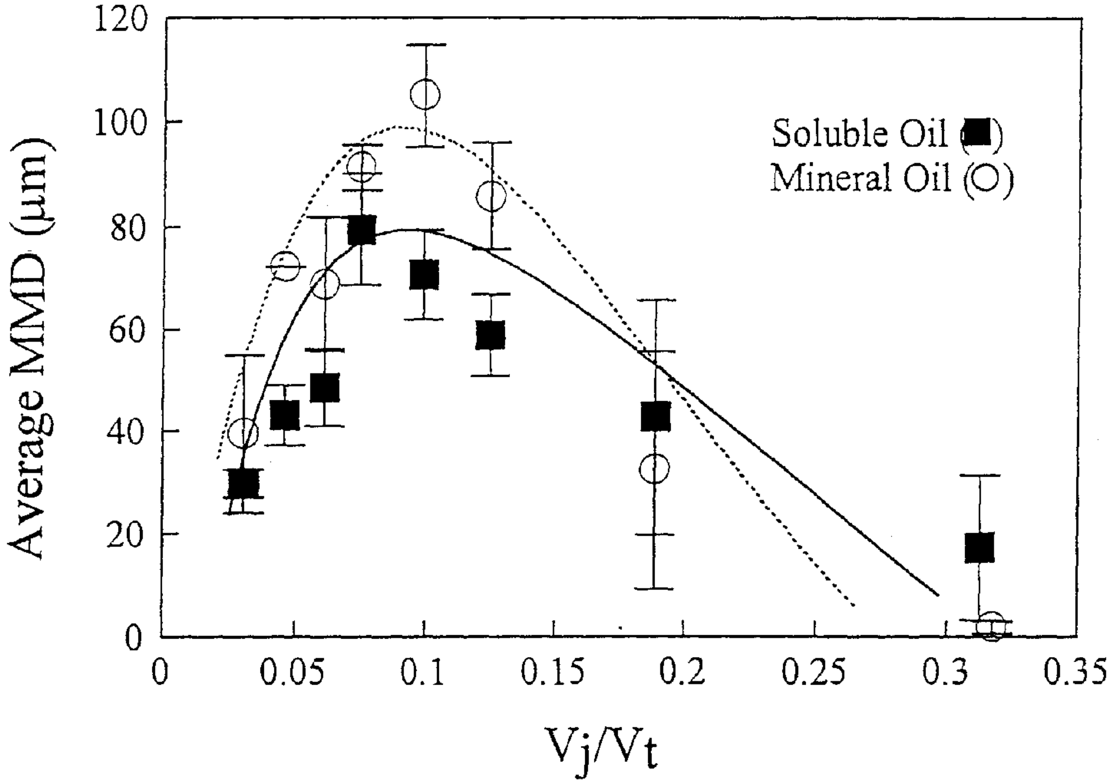

Figure 3.2: Average mass median diameters generated at different V_j/V_t ratios for soluble (□) and mineral oil (○). Error bars represent one standard deviation.

Table 3.4: Average geometric standard deviations, with standard error estimates, for soluble and low viscosity mineral oil mist generated by centrifugal force.

Fluid Type	# Observations	Average GSD
Soluble Oil	24	2.4 ± 0.05
Mineral Oil, low viscosity	30	2.3 ± 0.1

Table 3.5: Average mass median diameters and geometric standard deviations with standard error estimates from evaporation/condensation experiments.

Fluid Type	# Observations	Average MMD (μm)	Average GSD
Soluble Oil	30	3.2 ± 0.26	2.0 ± 0.05
Mineral Oil	19	2.1 ± 0.17	1.6 ± 0.04

3. Evaporation/Condensation

The average MMDs and GSDs of the mist generated by evaporation/condensation are listed in Table 3.5. Only metalworking fluid type affected the MMD and GSD. The average soluble oil MMD and GSD were larger than the average MMD and GSD for mineral oil.

Although none of the machining or fluid parameters except for metalworking fluid type affected the mist size distribution, additional insights come from plotting the MMD and GSD for soluble and mineral oil against the mist generation number, M, as shown in Figs. 3.3 and 3.4. The mist generation number is a dimensionless parameter that was defined in Chapter 2. Figures 3.3 and 3.4 show that the largest MMD and GSD result at the lowest mist generation number, M = 0.005. Otherwise, the MMD and GSD from the evaporation/condensation of both metalworking fluids were approximately constant.

F. Discussion

1. Impaction

The MMD of mineral oil mist generated by impaction increased as mineral oil viscosity decreased. Accordingly, soluble oil, with a viscosity much lower than mineral oil, should have produced the largest drops. However as shown in Table 3.3, the average MMDs of the soluble oil and high viscosity mineral oil were about the same. Since soluble oil contains more than 92% water and water has a high vapor pressure (2.5 kPa), the water fraction probably evaporated and reduced the soluble oil MMD to approximately the same size as that for high viscosity mineral oil.

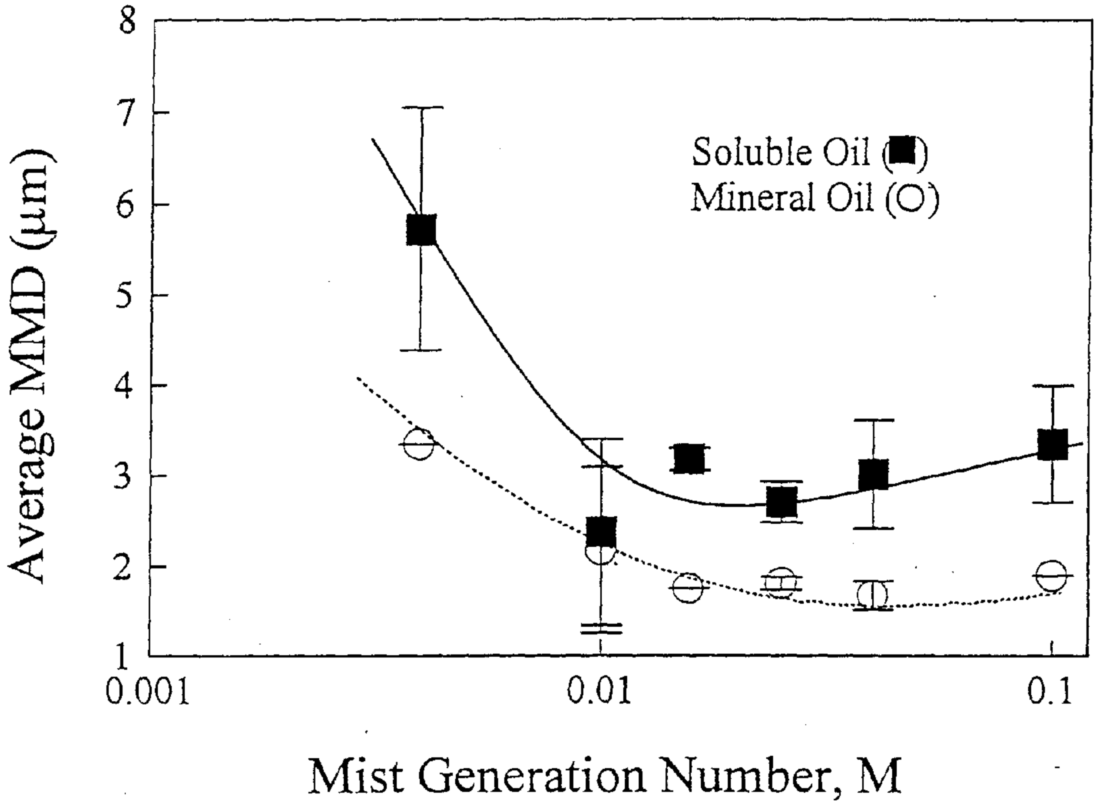

Figure 3.3: Mass median diameter as a function of mist generation number for soluble (□) and mineral oil (○). Error bars represent one standard deviation.

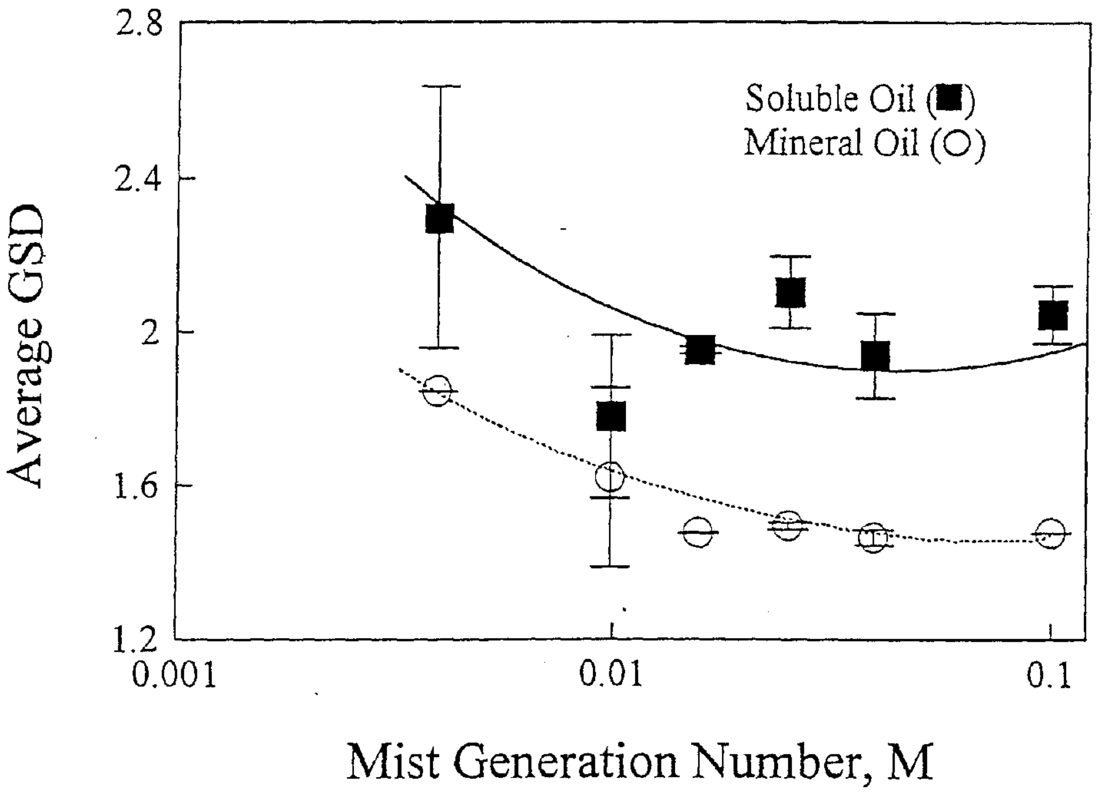

Figure 3.4: Geometric standard deviation versus mist generation number for soluble (□) and mineral oil (○). Error bars represent one standard deviation.

2. Centrifugal Force

The size distribution of the drops generated by centrifugal force resulted from two processes. In the first process, large primary drops were formed by the rotation of the aluminum rod, similar to rotary atomization by ligament formation (Kayano and Kamiya, 1978). The resulting Sauter mean diameter, SMD, of the primary drops can be calculated from:

$$SMD = 0.26\omega^{-0.79} Q_f^{0.32} D^{-0.69} \rho^{-0.29} \sigma^{0.26} (1 + 1.027\mu^{0.65}) \tag{3.1}$$

where ω is rotational speed, Q_f is fluid flow, D is the diameter of the rod, ρ is the fluid density, σ is the fluid surface tension, and μ is the fluid viscosity (Kayano and Kamiya, 1978). Mineral and soluble oil SMDs calculated from Eq. 3.1 are listed in Tables 3.6 and 3.7. For comparison to the data presented here, the SMDs in Table 3.7 and 3.7 were converted to MMDs using a relationship developed by Raabe (1971):

$$MMD = SMD \frac{\exp\left(3\ln^2(GSD)\right)}{\exp\left(2.5\ln^2(GSD)\right)} \tag{3.2}$$

where the GSD was calculated from the data collected during this work.

In the second process, the velocity imparted to the drops by the rotating rod caused them to collide with the housing walls or the lathe. This collision caused smaller, secondary drops to form if the dimensionless term, K, exceeded 57.7 (Mundo *et al.*, 1995), where

$$K = Oh\,Re^{1.25} = \left(\frac{\mu}{\sqrt{\rho\sigma d}}\right)\left(\frac{\rho v d}{\mu}\right)^{1.25}. \tag{3.3}$$

In Eq. 3.3, Oh is the Ohnesorge Number and Re is the Reynolds Number; μ is the fluid viscosity, ρ is the fluid density, σ is the fluid surface tension, d is the drop diameter, and v is the drop velocity. Once the threshold value of 57.7 is exceeded, the MMD of the secondary

Table 3.6: Calculated Sauter mean diameters, mass median diameters, and K values of mineral oil drops generated by centrifugal force.

V_j/V_t	SMD^A (μm)	MMD^B (μm)	K^C
0.03	173	251	81.8
0.05	255	369	59.3
0.07	216	313	96.6
0.08	290	420	65.3
0.10	318	461	69.9
0.13	342	495	73.8
0.19	606	878	35.4
0.32	714	1034	40.0

A: SMD calculated using Eq. 3.1
B: Conversion of SMD to MMD using Eq. 3.2
C: K-value calculated using Eq. 3.3

Table 3.7: Calculated Sauter mean diameters, mass median diameters, and K values of soluble oil drops generated by centrifugal force.

V_j/V_t	SMD[A] (μm)	MMD[B] (μm)	K[C]
0.03	161	233	104.9
0.05	237	343	76.0
0.07	201	291	123.9
0.08	269	390	83.6
0.10	295	428	89.5
0.13	317	459	94.5
0.19	563	815	45.3
0.32	663	959	51.3

A: SMD calculated using Eq. 3.1

B: Conversion of SMD to MMD using Eq. 3.2

C: K-value calculated using Eq. 3.3

drop size distribution decreases as K increases (Mundo *et al.*, 1995). For this research, values of K were calculated by substituting the primary droplet MMD calculated from Eqs. 3.1 and 3.2 as the drop diameter, d, and using the tangential velocity of the rotating aluminum rod as the drop velocity, v, as shown in Tables 3.6 and 3.7.

Using the data in Table 3.6 for mineral oil and Table 3.7 for soluble oil, a qualitative analysis of Fig. 3.2 is possible by dividing the V_j/V_t ratios into three groups.

First, V_j/V_t ratios less than 0.07 corresponded to low fluid flows and high rotational speeds. From Eqs. 3.1 and 3.2, the calculated MMD of the primary drops generated by the rotation of the aluminum rod was less than 250 μm. The secondary drops formed by the collision of the primary drops with the walls had small diameters because of their high K value. Thus, the measured MMDs of the overall size distribution at low V_j/V_t ratios were less than 50 μm for soluble oil and less than 80 μm for mineral oil.

For V_j/V_t ratios between 0.07 and 0.13, the MMDs of the primary drops calculated from Eqs. 3.1 and 3.2 were between 300 μm and 500 μm. Because the corresponding K values in Table VI decreased as the V_j/V_t ratios increased, the collision of the primary drops with the housing walls generated larger secondary drops. The larger primary and secondary drops caused the largest average MMDs for the total size distributions measured by the Aerosizer LD, as shown in Fig. 3.2.

Figure 3.2 also shows that the measured soluble oil MMD was less than the measured MMD for mineral oil as long as the V_j/V_t ratio was less than 0.13. At Vj/Vt ratios less than 0.13, the primary soluble oil drops were smaller than the primary mineral oil drops, and the

K value for the formation of the secondary soluble oil drops was greater than the K value for mineral oil.

When the V_j/V_t ratio was greater than 0.19, the MMDs of the soluble and mineral oil primary drops calculated from Eqs. 3.1 and 3.2 were greater than 800 μm. These primary drops were too large to be measured by the Aerosizer (API, 1995) or gravitationally settled before being sampled. In addition, these drops did not break apart upon colliding with the walls because their K values did not exceed 57.7. Hence, the Aerosizer LD probably sampled only the lower end of the mist size distribution, so that the resulting measured MMDs for soluble and mineral oil at high V_j/V_t ratios were lower, between 5 and 40 μm. At V_j/V_t ratios greater than 0.13, the soluble oil MMDs were larger than those for mineral oil because the Aerosizer LD may have sampled the smaller soluble oil drops more efficiently.

Centrifugal force experiments with high viscosity mineral oil did not yield similar variations in MMD at different V_j/V_t ratios. Using Eqs. 3.1 and 3.2, the calculated MMD of the high viscosity mineral oil drops formed by the rotating cylinder was greater than 1000 μm. In addition, secondary drop formation did not occur because the K value was less than 57.7 at both V_j/V_t ratios. Therefore, the Aerosizer LD only sampled the lower end of the size distribution, as discussed in the preceding paragraph.

The combination of the primary and secondary drop formation processes caused the GSD for mineral and soluble oil to remain roughly constant for all V_t/V_j ratios. The wide range of drop sizes generated by the rotation of the aluminum rod and the collisions with the walls homogenized the breadth of the size distribution.

For all V_t/V_j ratios, evaporation of the water fraction of the soluble oil drops was not important because the relative humidity inside the chamber reached 100% less than thirty seconds into a three-minute experiment.

3. Evaporation/Condensation

Figures 3.3 and 3.4 show that the soluble oil MMD and GSD were always larger than those for mineral oil at the same mist generation number. Chapter 3 showed that mineral oil produced more drops than soluble oil at the same machining conditions. Because fewer soluble oil drops were generated during machining, there were fewer sites on which the soluble oil vapor could condense, causing the soluble oil drop MMD and GSD to be larger.

As shown in Fig. 3.3, the MMD of the mist generated by evaporation/ condensation was independent of the mist generation number except when M was low, around 0.005. Tukey tests confirmed that the lowest mist generation number produced significantly larger MMDs and GSDs for soluble and mineral oil. When M was about 0.005, less mist was generated so that fewer drops were available for the vaporized oil to condense on, causing the MMD and GSD for soluble and mineral oil to increase.

For mist generation numbers greater than 0.005, factors besides the other machining or fluid parameters determined the size distribution of the mist generated. For example, coagulation of the drops within the chamber probably increased the uniformity of the mist size distribution. Higher rotational speeds increased the turbulence within the chamber, promoting coagulation and the mass transfer of oil vapor to the drops. Also, the rate of condensation would affect the mist size distribution. Condensation rate was dependent on the drop diameter, actual vapor pressure of each oil component, saturated vapor pressure of each component, ambient temperature, diffusion coefficient, density, and molecular weight

(Maxwell, 1994). In addition, the environment within the chamber was constantly changing during the machining process. Fresh metalworking fluid was applied and vaporized continuously. As a result, the number of drops in the chamber increased as the oil vapor condensed. Since the mass generation rate increased with mist generation number but the drop size distribution did not change significantly for mist generation numbers greater than 0.005, the number of drops generated must have increased instead of drop size.

G. Conclusions

Of the three formation mechanisms, evaporation/condensation generated the smallest drops, whereas centrifugal force produced the largest drops. The concentration of small metalworking fluid drops in industrial environments will be regulated if the PEL change NIOSH recommended is adopted. However, this work shows that altering machining practices or changing fluid parameters will not affect the size distribution of the mist generated by evaporation/ condensation. Extremely large drops produced by centrifugal force are removed efficiently by mist collectors and gravitationally settle quickly before posing a threat to worker health.

The size distribution data collected during this study can be applied directly to similar machines only. Industrial facilities may use different machining conditions and fluid flows. Accordingly, the mist size distribution may vary for larger lathes or different types of machines. In addition, the degree of enclosure around a machine and ambient conditions within the facility will influence rate of evaporation and change the resultant mist size distribution. Nevertheless, the processes affecting mist size distribution should be the same as those investigated here, so that insights concerning the mist size distribution discussed in this paper should be applicable to other operations or conditions.

The results of this research can be applied to improve the operation of control equipment and local exhaust ventilation. For enclosed machines connected to a mist collector, minimizing evaporation to keep drops as large as possible will increase collector efficiency. Enclosing machines will maintain a high vapor concentration, decrease drop evaporation, and maintain drop size. When an enclosed machine is not in use, turning off its exhaust system will help prevent the dilution of the vapor concentration within the connected exhaust duct.

REFERENCES

Ameille, J., Wild, P., and Choudat, D., "Respiratory Symptoms, Ventilatory Impairment, and Bronchial Reactivity in Oil Mist Exposed Automobile Workers," *Amer. J. Ind. Med.*, 27:247-256, 1995.

American Conference of Governmental Industrial Hygienists (ACGIH), 1998 TLVs and BEIs: Threshold Limit Values for Chemical Substance and Physical Agents, ACGIH, Cincinnati, OH, 1998.

Beattie, P.J., Strohm, B.H., "Health and Safety Aspects in the Use of Metalworking Fluids," Metalworking Fluids, editor: J.P. Byers, Marcel Dekker, New York, 1994.

Bennett, E.O., Bennett, D.L., "Minimizing Human Exposures to Chemicals in Metalworking Fluids," *Lubrication Engineering*, 43:167-175, 1987.

Bhunia, S.K., and Lienhard, V.J.H., "Surface Disturbance Evolution and the Splattering of Turbulent Liquid Jets," *ASME J. Fluids Eng*, 116:721-727, 1994.

Booser, E.R., editor: CRC Handbook of Lubrication (Theory and Practice of Tribology) Volume II: Theory and Design, CRC Press Inc., Boca Raton, FL, 1984.

Byers. J.P., "Laboratory Evaluation of Metalworking Fluids," Metalworking Fluids, editor: J.P. Byers, Marcel Dekker, New York, 1994.

Chan, T.L., D'Arcy, J.B., and Siak, J., "Size Characteristics of Machining Fluid Aerosols in an Industrial Metalworking Environment," *Appl. Occup. Environ. Hyg.*, 5:162-170, 1990.

Chen, B.T., "Instrument Calibration," Aerosol Measurement: Principles, Techniques, and Applications, editors: K. Willeke and P.A. Baron, Van Nostrand Reinhold, New York, pp. 503, 1993.

Childs, T.H.C., Maekawa, K., and Maulik, P., "Effect of Coolant on Temperature Distribution in Metal Machining," *Mater. Sci. & Technol.*, 4:1006-1019, 1988.

Cooper, S.J., Raynor, P.C., and Leith, D., "Evaporation of Mineral Oil in a Mist Collector," *Appl. Occup. Environ. Hyg.*, 11:1204-1211, 1996.

De Boer, E.M., Van Ketel, W.G., and Bruynzeel, D.P., "Dermatoses in Metal Workers (I). Irritant Contact Dermatitis," *Contact Dermatitis*, 20:212-218, 1989a.

De Boer, E.M., Van Ketel, W.G., and Bruynzeel, D.P., "Dermatoses in Metal Workers (II). Allergic Contact Dermatitis," *Contact Dermatitis*, 20:280-286, 1989b.

Decoufle, P., "Further Analysis of Cancer Mortality Patterns Among Workers Exposed to Cutting Oil Mists," *J. National Cancer Institute*, 61:1025-1030, 1978.

Diamond, W.J., Practical Experiment Designs for Engineers and Scientists, Wadsworth Inc., Belmont, CA, 1981.

Eisen, E.A., Tolbert, P.E., Monson, R.R., and Smith, T.J., "Mortality Studies of Machining Fluid Exposure in the Automobile Industry (I). A Standardized Mortality Ratio Analysis," *Amer. J. Ind. Med.*, 22:809-824, 1992.

Eisen, E.A., Tolbert, P.E., Hallock, M.H., Monson, R.R., Smith, T.J., and Woskie, S.R., "Mortality Studies of Machining Fluid Exposure in the Automobile Industry (III). A Case Control Study of Larynx Cancer," *Amer. J. Ind. Med.*, 26:185-202, 1994.

Frazier, A.D., "Cutting Fluid Applications for Today's Materials," Improving Production with Coolants and Lubricants, 1st ed., editor: D.C. Zintak, SME, Dearborn, MI, 1982.

Hallock, M.F., Smith T.J., Woskie, S.R., and Hammond, S.K., "Estimation of Historical Exposures to Machining Fluids in the Automotive Industry," *Amer. J. Ind. Med.*, 26:621-634, 1994.

Jarvholm, B., Fast, K., Lavenius, B., and Tomsic, P., "Exposure to Cutting Oils and its Relation to Skin Tumors and Premalignant Skin Lesions on the Hands and Forearms," *Scand. J. Work Environ. Health*, 11:365-369, 1985.

Jarvholm, B., Lavenius, B., "Mortality and Cancer Morbidity in Workers Exposed to Cutting Fluids," *Archives of Environmental Health*, 42:361-365, 1987.

Jarvholm, B., Easton, D., "Models for Skin Tumor Risks in Workers Exposed to Mineral Oils," *British Journal of Cancer*, 62:1039-1041, 1990.

Kayano, A., and Kamiya, T., "Calculation of the Mean Size of the Droplets Purged from the Rotating Disk," Proceedings of the 1st International Conference on Liquid Atomization and Sprays, Tokyo, 1978, pp. 133-143, 1978.

Kennedy S.M., Greaves, I.A., Eisen, E.A., Smith, T.J., Woskie, S.R., "Acute Pulmonary Responses Among Automobile Workers Exposed to Aerosols of Machining Fluids," *Amer. J. Ind. Med.*, 15:627-641, 1989.

Konrad, G., Biedermann, M., and Caramanschi, A., "LC-GC Analysis of the Aromatics in a Mineral Oil Fraction: Batching Oil for Jute Bags," *J. High Res. Chrom.*, 14:33-39, 1991.

Leep, H.R., "Metal Cutting Processes," Metalworking Fluids, editor: J.P. Byers, Marcel Dekker, New York, 1994.

Leith, D., Raynor, P.C., Boundy, M.G., and Cooper, S.J., "Performance of Industrial Equipment to Collect Coolant Mists," *Am. Ind. Hyg. Assoc. J.*, 57:1142-1148, 1996.

Lide D.R., editor, CRC Handbook of Chemistry and Physics, 78th edition, CRC Press, New York, New York, 1997.

Mackerer, C.R., "Health Effects of Oil Mists: A Brief Review," *Tox. and Ind. Health*, 5:429-440, 1989.

Maxwell, J.C., In: Aerosol Science and Technology, P.C. Reist, McGraw-Hill, Inc., New York , 1993.

McKee, R.H., O'Connor, D.J., "Dermal Carcinogenicity Studies of Metalworking Fluids," *Lubrication Engineering*, 52:97-102, 1996.

Mundo, CH., Sommerfeld, M., and Tropea, C., "Droplet-Wall Collisions: Experimental Studies of the Deformation and Breakup Process," *Int. J. Multiphase Flow,* 21:151-173, 1995.

National Institute for Occupational Safety and Health (NIOSH), *National Occupational Hazard Survey*, vol. III (DHHS/NIOSH publ. No. 78-114), Cincinnati, OH, 1977, pp. 216-219.

National Institute for Occupational Safety and Health (NIOSH), *Occupational Exposure to Metalworking Fluids*, (DHHHS/NIOSH publ. No.98-102), Cincinnati, OH, 1998.

National Institute for Occupational Safety and Health (NIOSH), *Collaborative Testing of Activated Charcoal Sampling Tubes for Seven Organic Solvents*, (DHHHS/NIOSH publ. No.75-184), Cincinnati, OH, 1975.

Oberg, E., Jones, F.D., and Horton, H.L., Machinery's Handbook, 22nd edition, H.H. Ryffel, editor, Industrial Press, Inc., New York, New York, 1984.

Park, R.M., Wegman, D.H., Silverstein, M.A., Maizlish, N.A., and Mirer, F.E., "Causes of Death Among Workers in a Bearing Manufacturing Plant," *Amer. J. Ind. Med.*, 26:449-463, 1988.

Park, R.M., and Mirer, F.E., "A Survey of Mortality at Two Automotive Engine Manufacturing Plants," *Amer. J. Ind. Med.*, 30:664-673, 1996.

Perry, R.H. and Green, D.W., editors, Perry's Chemical Engineers Handbook, 7th edition, McGraw-Hill, New York, New York, 1997.

Raabe, O.G., "Particle Size Analysis Utilizing Grouped Data and the Log-Normal Distribution," *J. Aerosol Sci.*, 2:289-303 (1971).

Robertson, A.S., Weir, D.C., and Burge, P.S., "Occupational Asthma Due to Oil Mists," *Thorax*, 43:200-205, 1988.

Robins, T.G., Seixas, N.S., Burge, H., Abrams, L., and Minick., S., "Association of Cross-Shift Decrements in Pulmonary Function with Machining Fluid Exposure," *Amer. J. Respir. Crit. Care Med.*, 151:A420, 1995.

Silverman, D.T., Hoover, R.N., Albert., S., and Graff, K.M., "Occupational Risks of Bladder Cancer in the United States: White Men," *J. National Cancer Institute*, 81:1472-1479, 1989.

Silverstein, M.A., Park, R.M., Marmor, M., Maizlish, N.A., and Mirer, F.E., "Mortality Among Bearing Plant Workers Exposed to Metalworking Fluids and Abrasives," *J. Occup. Med.*, 30:706-714, 1988.

Smolenski, J.M., Gulari, E., and Manke, C.W., "Atomization of Dilute Polyisobutylene/Mineral Oil Solutions," *AIChE Journal*, 42:1201-1212, 1996.

Springborn, R.K., editor: Cutting and Grinding Fluids: Selection and Application, ASTME, Dearborn, MI, 1967.

Thornburg, J., Cooper, S., and Leith, D., "Counting Efficiency of the API Aerosizer," *J. Aerosol Sci.*, in press.

Tolbert, P.E., Eisen, E.A., Pothier, L.J., Monson, R.R., Hallock, M.H., and Smith, T.J., "Mortality Studies of Machining Fluid Exposure in the Automobile Industry," *Scand. J. Work Environ. Health*, 18:351-360, 1992.

Vincent, J., Aerosol Science for Industrial Hygienists, Pergamon, New York, 1995.

Wagner, W. D., Wright, P.G., and Stokinger, H.E., "Inhalation Toxicology of Oil Mists (I). Chronic Effects of White Mineral Oil," *Industrial Hygiene Journal*, 25:158-167, 1964.

Woskie, S.R., Smith, T.J., Hammond, K., Hallock, M.H., Rosenthal, F., Eisen, E.A., Kriebel, D., and Greaves, I.A., "Size-Selective Pulmonary Dose Indices for Metal-Working Fluid Aerosols in Machining and Grinding Operations in the Automobile Manufacturing Industry," *Amer. Ind. Hyg. Assoc. J.*, 55:20-29, 1994a.

Woskie, S.R., Smith, T.J., Hammond, K., and Hallock, M.H., "Factors Affecting Worker Exposures to Metal-Working Fluids During Automotive Component Manufacturing," *Appl. Occup. Environ. Hyg.*, 9:612-621, 1994b.

Yaws, C.L., Handbook of Vapor Pressure, Vol. 3, Gulf Publishing Co., Houston, Texas, 1994.

PUBLICATIONS

The work presented in this report and additional research resulting from this project has been presented at several conferences and submitted for publication in peer reviewed journals. A list of all presentations and manuscripts is listed below.

Presentations

"Modeling Mist Generation During Metal Machining," platform presentation, American Association of Aerosol Research, 17th Annual Meeting, Cincinnati OH, 1998.

"Mist Generation During Machining Operations," platform presentation, Purdue Industrial Waste Conference, West Lafayette, IN, 1998.

"Mist Formation During Metal Machining," poster presentation, American Association of Aerosol Research, 16th Annual Meeting, Denver CO, 1997.

"Factors Influencing Mist Generation During Machining," poster presentation, Metalworking Fluid Symposium II, American Automobile Manufacturers Association, Detroit MI, 1997.

Publications

Thornburg, J., Cooper, S., and Leith, D.; "Counting Efficiency of the API Aerosizer;" *Journal of Aerosol Science*, in press.

Thornburg, J., and Leith, D.; "Mist Generation During Metal Machining;" submitted to *Journal of Tribology*.

Thornburg, J., and Leith, D.; "Size Distribution of Mist Generated During Metal Machining;" submitted to *Annals of Occupational and Environmental Hygiene*.